# FREEZE, PROMPT, AND ADAPT: A FRAMEWORK FOR SOURCE-FREE UNSUPERVISED GNN PROMPTING

**Anonymous authors**
Paper under double-blind review

## ABSTRACT

Prompt tuning has become a key mechanism for adapting pre-trained Graph Neural Networks (GNNs) to new downstream tasks. However, existing approaches are predominantly supervised, relying on labeled data to optimize the prompting parameters and typically fine-tuning a task-specific prediction head—practices that undermine the promise of parameter-efficient adaptation. We propose *Unsupervised Graph Prompting Problem (*UGPP*)*, a challenging new setting where the pre-trained GNN is kept entirely frozen, labels on the target domain are unavailable, the source data is inaccessible, and the target distribution exhibits covariate shift. To address this, we propose UGPROMPT, the first fully unsupervised GNN prompting framework. UGPROMPT leverages consistency regularization and pseudo-labeling to train a prompting function, complemented with diversity and domain regularization to mitigate class imbalance and distribution mismatch. Our extensive experiments demonstrate that UGPROMPT consistently outperforms state-of-the-art supervised prompting methods with access to labeled data, demonstrating the viability of unsupervised prompting as a practical adaptation paradigm for GNNs.

## 1 INTRODUCTION AND RELATED WORK

Prompt tuning Li & Liang (2021); Lester et al. (2021) has driven many recent developments for Large Language Models (LLMs). These methods optimize external prompting parameters to guide a model's responses. The goal is to avoid fine-tuning the model's vast number of internal parameters for adaptation to new downstream tasks, keeping the core pre-trained knowledge intact Zheng et al. (2025); Han et al. (2024); Liu et al. (2023a). However, prompting becomes more challenging for graphs because: First, there is a wide range of graph tasks; thus, unlike general language tasks Devlin et al. (2019); Radford & Narasimhan (2018), *task unification* is difficult in graphs. Subsequently, it restricts the opportunities of collecting large amounts of data easily from available resources such as the internet Radford et al. (2019) and causes bottlenecks to pre-train *large* Graph Neural Networks (GNNs) for general purposes. Second, because of the limited reasoning capabilities of GNNs Morris et al. (2024); Mao et al. (2024a) it is non-trivial to constitute instructive graph prompts by the human (natural) language Fatemi et al. (2024).

A few recent studies have adopted prompting for GNNs to align the objectives of pre-training on source data and fine-tuning on target data, mostly following the "pre-train, prompt, fine-tune" pipeline Sun et al. (2022). These works design unified tasks that allow optimizing a GNN with semantically similar objectives on the pretext and downstream tasks Huang et al. (2023); Liu et al. (2023b); Fang et al. (2023); Sun et al. (2023); Yu et al. (2024b); Chen et al. (2025). However, the current GNN prompting paradigm suffers from two key limitations that hinder its efficiency compared to its LLM counterparts. First, the existing methods rely heavily on labeled data—which is costly to obtain—to achieve competitive performance. Second, they require training new projection heads for each downstream task, a form of *lightweight fine-tuning* Li & Liang (2021). These dependencies on additional parameters and labeled data (especially in scenarios where the original source data is inaccessible, e.g., due to privacy) prevent GNNs from being used as truly frozen models. This gap motivates our work to establish a more practical and efficient prompting paradigm for GNNs.

To directly address these limitations, we first introduce the Unsupervised Graph Prompting Problem (**UGPP**), a rigorous novel problem formulation. The UGPP setup evaluates a method under four key

conditions: the GNN's parameters are frozen, there is a covariate shift in the target data distribution, no target labels are available for adaptation, and the source data is inaccessible. While this setup shares similarities with Unsupervised Source-Free Domain Adaptation (SFDA) Li et al. (2024), it differs in a crucial aspect: UGPP requires the entire pre-trained GNN to be frozen, whereas SFDA methods Mao et al. (2024b); Zhang et al. (2024) rely on fine-tuning the model's parameters. This setting firmly places our work within the paradigm of parameter-efficient prompting, rather than full model adaptation.

Within this challenging setup, we propose UGPROMPT, the first fully unsupervised GNN prompting framework. UGPROMPT trains a prompting function using consistency regularization and confident pseudo-labeling, enabling the frozen GNN to adapt its knowledge to the new target distribution. To ensure robustness, we introduce two additional regularization techniques: one to counteract prediction bias from class imbalance and another to make the prompted graphs close to the original data distribution. Our extensive experiments show that UGPROMPT, despite being fully unsupervised, consistently outperforms state-of-the-art (SOTA) prompting methods that have the advantage of full access to labeled data. Our major contributions are summarized as follows.

- **Problem formulation.** We propose UGPP, a challenging problem setup that isolates the true effectiveness of a prompting function by disallowing any updates to the pre-trained GNN's parameters.
- **Novel unsupervised methodology.** We propose UGPROMPT, the first fully unsupervised GNN prompting method that leverages consistency regularization and pseudo-labeling to adapt a frozen GNN to new data distributions.
- **Empirical analysis.** We demonstrate that UGPROMPT substantially outperforms supervised SOTA methods on node and graph classification tasks, validating the effectiveness of unsupervised adaptation in this novel and more practical setting.

## 2 BACKGROUND & PROBLEM FORMULATION

Previous studies on adapting prompt tuning for GNNs use lightweight fine-tuning Li & Liang (2021); Lester et al. (2021) with supervision which has been addressed widely in different domains such as computer vision van den Oord et al. (2018); Chen et al. (2020); Zhuang et al. (2021) and NLP Devlin et al. (2019); Ruder et al. (2019). Specifically, recent works have followed the *"pre-train, prompt, fine-tune"* setup Sun et al. (2022); Liu et al. (2023b); Sun et al. (2023); Fang et al. (2023). In this section, we first introduce this setting and discuss its limitations, then we introduce our proposed problem setting which addresses these limitations.

### 2.1 PRE-TRAIN, PROMPT, FINE-TUNING

This pipeline aims to bridge the generalization gap of pre-trained GNNs being applied to the downstream tasks that semantically differ from the pretext tasks. Unlike the traditional supervised and "pre-training, fine-tuning" methods, this pipeline employs a task unification step before pre-training and fine-tuning. This is essential as it helps align the pretext and downstream objectives to optimize a pre-trained model on new datasets. The steps are as follows.

*(1) Pre-train.* Formally, given a set of tuples $\mathcal{S} = \{(\mathcal{T}_i, \mathcal{D}_i)\}_{i=1}^{N_s}$, with $N_s$ samples, from pretext task $\mathcal{T}_i$ and dataset $\mathcal{D}_i$, first all the tasks are unified to task $\mathcal{T}_u$ and the corresponding changes apply for their associated datasets to make a new set $\mathcal{S}_u = \{(\mathcal{T}_u^i, \mathcal{D}_u^i)\}_{i=1}^{N_s}$. Then a GNN encoder $g(.;\theta_g)$ is pre-trained on $\mathcal{S}_u$ using a unsupervised approach such as contrastive learning You et al. (2020); Xia et al. (2022). For downstream tasks, by adding a projection head $h(.;\theta_h)$ after the encoder, a model $\psi = h \circ g$ is formed of which the encoder parameters $\theta_g$ are frozen, and only the head parameters $\theta_h$ will be trained. *(2) Prompting.* At this stage, a prompting function $f(.,\theta_f)$ is employed to construct a prediction model $\varphi$. The prompting function is either a prefix module, i.e., $\varphi = h \circ g \circ f$, or a postfix one, i.e., $\varphi = f \circ h \circ g$. *(3) Fine-tuning.* In the final step, the set of parameters $\{\theta_h, \theta_f\}$ of $\varphi$ are optimized for every unified downstream task $\mathcal{T}_u$ with the new labeled samples.

*Limitations.* A deeper look at the *"pre-train, prompt, fine-tune"* pipeline reveals that although the current methods impose less trainable parameters compared to full fine-tuning (fine-tuning both pre-trained feature encoder and decoder), they involve partial (lightweight) fine-tuning Han et al. (2024);

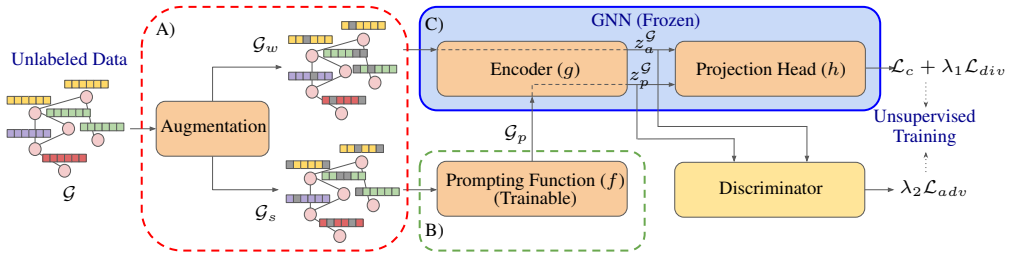


Figure 1: Overview of UGPROMPT. A) A non-parametric algorithm generates a weak augmentation $\mathcal{G}_w$ and a strong augmentation $\mathcal{G}_s$ from an unlabeled graph $\mathcal{G}$. B) The learnable prompting function $f$ generates a prompted graph $\mathcal{G}_p$ from $\mathcal{G}_s$. C) The base GNN with frozen parameters scores $\mathcal{G}_p$ and $\mathcal{G}_w$. A discriminator taking input from the latent representation ($z_a^{\mathcal{G}}$ for $\mathcal{G}_w$ and $z_p^{\mathcal{G}}$ for $\mathcal{G}_p$) of the GNN's encoder regularizes the model to adapt to the input distribution.

Li & Liang (2021); Lester et al. (2021), as they also train the GNN's decoder (projection head) along with the new parameters of the prompting function. Subsequently, labels become essential for this partial fine-tuning, and they are unable to leverage unlabeled data from large datasets when collecting labeled data is challenging Radford et al. (2019). Also, fine-tuning a large model that is pre-trained on large datasets may inject noisy information when the labeled downstream datasets are small Bousquet et al. (2004); Shalev-Shwartz & Ben-David (2014). Therefore, it reduces the model generalization when it comes to diverse applications Brown et al. (2020).

### 2.2 OUR PROBLEM SETTING

To address the above limitations, we first need a suitable problem setting that offers insights into how well a prompting method performs when there is lack of labeled data. It is also crucial to evaluate if the method generalizes across tasks without fine-tuning the base GNN model parameters.

**Unsupervised Graph Prompting Problem (UGPP).** *Suppose a GNN model* $\varphi(.;\theta_g,\theta_h) = h(.;\theta_h) \circ g(.;\theta_g)$ *is given, where* $g$ *and* $h$ *are its encoder and decoder. Also,* $\varphi$ *is pre-trained for task* $\mathcal{T}$ *on a labeled source dataset* $\mathcal{D}_s = \{(x_s^i, y_s^i) : x_s^i \sim \mathcal{P}_X^s,\ y_s^i \sim \mathcal{P}_{Y|X}^s\}_{i=1}^{N_s}$*, where* $x_s^i$ *is a sample (e.g., a graph or node), and* $y_s^i$ *is its associated label. The problem is to train a prompting module* $f(.;\theta_f)$ *on an unlabeled target dataset* $\mathcal{D}_t = \{x_t^j : x_t^j \sim \mathcal{P}_X^t\}_{j=1}^{N_t}$*, s.t.* $\mathcal{P}_X^s \neq \mathcal{P}_X^t$*, to enhance the performance of* $\varphi$ *for task* $\mathcal{T}$ *on* $\mathcal{D}_t$*, assuming* $\theta_g$ *and* $\theta_h$ *are fixed and* $\mathcal{D}_s$ *is unobservable. Further, assume* $\mathcal{P}_{Y|X}^t$ *is unobserved but* $\mathcal{P}_{Y|X}^t = \mathcal{P}_{Y|X}^s$.

This problem, UGPP, focuses on prompting without labeled data. A prompting method performing well in this setting has three advantages: *First,* it is model and task agnostic, i.e., this method works for conventional GNNs (e.g., GCN, GAT) and tasks (e.g., node/graph classification). *Second,* it is unsupervised, so a large number of datasets can be utilized to improve generalization. *Third,* this setting does not depend on the source data. This is particularly beneficial when the source data is inaccessible, e.g. due to privacy issues.

It is noteworthy that our setting fundamentally differs from conventional Unsupervised SFDA settings. While SFDA typically involves fine-tuning the parameters of the source-trained model, our setting mandates that the pre-trained GNN remains entirely frozen. All adaptation is achieved exclusively by optimizing the external prompt parameters. Please find additional discussions on the UGPP definition in Appendix A.4. Nevertheless, we compare our proposed method (described next) against recent graph SFDA methods in Appendix A.7.4.

## 3 OUR METHOD: UGPROMPT

Here, we introduce UGPROMPT, an unsupervised GNN prompting method, to address UGPP.

**Motivation.** We aim to design an unsupervised prompting framework that helps a pre-trained GNN make robust predictions while its parameters are frozen. To achieve this, we take advantage of pseudo-labeling Lee (2013); Xie et al. (2020) and consistency regularization Sajjadi et al. (2016); Laine & Aila (2017). To train a prompting function in a fully unsupervised manner, UGPROMPT

first obtains randomly augmented graphs from the target dataset. Then we employ consistency regularization Zhang et al. (2021); Wang et al. (2023), where certain predictions of the base GNN are filtered by a confidence threshold and exploited as pseudo-labels for optimization. Indeed, the knowledge learned from the source dataset is used to reduce prediction entropy and handle distribution shifts by relying on the GNN's confident predictions for unlabeled target data. The prompting module enhances target input samples by adding key information to make them more similar to source samples. Empirical evidence to support this claim is in the Appendix A.7.5. We describe our framework (Figure 1) for graph-level tasks. Note that it also generalizes to node-/edge-level tasks.

**Overview of UGPROMPT.**Our framework to address UGPP has a training and an inference step. The training step involves two components: *consistency-based prompting* and *prompt regularization*. *Consistency-based prompting* starts with augmenting each input graph twice, with one of them being modified by a prompting function. Next, the GNN scores both samples. The objective is to train the prompting function such that the GNN produces "consistent prediction scores" for both samples of this pair with a certain confidence. In *prompt regularization* we introduce two regularization techniques: one to tackle biased predictions caused by a class imbalance in the data and another to prevent generating out-of-distribution (OOD) prompted graphs. During inference, a test graph is fed to the prompting function without augmentation and its output goes to the GNN. We discuss a task unification step to generalize on other graph tasks, e.g. node-classification, in Appendix A.5.3.

### 3.1 THE CONSISTENCY-BASED PROMPTING

Our prompting method is designed to reduce the discrepancy of the base GNN predictions over random augmentations of the same input graphs. We achieve this without labels by utilizing an algorithmic augmentation step, and then generating pseudo-labels out of the unlabeled augmentations when their assigned scores by the GNN meet a certain confidence threshold. We provide the details of these two stages below.

***Algorithmic augmentation.*** Consistency regularization techniques Zhang et al. (2021) train *strong augmentations* of samples using the pseudo-labels derived from their *weak augmentations*. Since our focus is on optimizing the prompting module rather than fine-tuning the base GNN, we adopt this technique as follows. We use a random non-parameterized augmentation algorithm (we use random feature masking in our experiments). More specifically, we mask a group of features with a certain probability. We augment an input graph $\mathcal{G}$ to create a weak augmentation $\mathcal{G}_w$ with masking probability $p_w$ and also a strong augmentation $\mathcal{G}_s$ with probability $p_s$, where $p_s > p_w$. We pass $\mathcal{G}_s$ through a learnable prompting function $f(.;\theta_f)$ to obtain a *prompted graph* $\mathcal{G}_p = f(\mathcal{G}_s;\theta_f)$. We keep $\mathcal{G}_w$ unchanged and call it a *non-prompted* augmentation graph.

***Learnable prompting.*** We use a prefix prompting module to transform input samples for the base GNN. Our approach is generic enough to allow the integration of different prompting functions. For our experiments, we choose a function $f$ that enriches the feature vectors of nodes since this particular design aligns with our augmentation technique of random feature masking. This way of adding learnable parameters is used in GPF-Plus Fang et al. (2023).

Specifically, we learn a prompting function $f$ with parameter set $\theta_f = \{t_j^* : t_j^* \in \mathbb{R}^d\}_{j=1}^{N^*}$. For input graph $\mathcal{G}$ of $N$ nodes with nodes features set $X = \{x_i : x_i \in \mathbb{R}^d\}_{i=1}^{N}$, the function $f$ makes prompted graph $\mathcal{G}_p$ with feature set $X_p = \{x_i + t_i : x_i \in X,\ x_i, t_i \in \mathbb{R}^d\}_{i=1}^{N}$ such that $t_i = \sum_{j=1}^{n_t} \alpha_{i,j} t_j^*$ and $\alpha_{i,j} = \frac{\exp(x_i^T t_j^*)}{\sum_{l=1}^{n_t} \exp(x_i^T t_l^*)}$ .

***Consistency-based Objective.*** We optimize $\theta_f$ to minimize the discrepancy between the GNN's prediction scores for the non-prompted augmented graph $\mathcal{G}_w$ and the prompted graph $\mathcal{G}_p$. This would lower the entropy of the GNN's scores for the target unlabeled data. Intuitively, a well-trained frozen GNN model $\varphi$ makes accurate predictions for samples close to the source distribution. Therefore, as training proceeds and $\varphi$ scores different random perturbations of the same samples, we utilize its confident predictions as pseudo-labels for optimization, as this helps $f$ to capture the distribution shift and make the predictions robust. We achieve this by passing $\mathcal{G}_p$ and $\mathcal{G}_w$ to $\varphi$ for prediction as:

$$\tilde{p}_{\varphi}^{\mathcal{G}}(y) = \delta(h(z_a;\theta_h)) \qquad \hat{p}_{\varphi}^{\mathcal{G}}(y) = \delta(h(z_p;\theta_h)) \tag{1}$$

where $z_a^{\mathcal{G}} = g(\mathcal{G}_w; \theta_g)$ and $z_p^{\mathcal{G}} = g(\mathcal{G}_p; \theta_g)$, $\delta(.)$ denotes the softmax function, $\tilde{p}_\varphi^{\mathcal{G}}(y), \hat{p}_\varphi^{\mathcal{G}}(y) \in \mathbb{R}^C$, and $C$ is the number of classes. Pseudo-labels are made as $\mathbf{p}_\varphi^{\mathcal{G}}(y) = \arg\max \tilde{p}_\varphi^{\mathcal{G}}(y)$, and finally, the consistency loss is:

$$\mathcal{L}_c = \frac{1}{|\mathcal{B}|} \sum_{\mathcal{G} \in \mathcal{B}} \mathbb{1}(\max(\tilde{p}_\varphi^{\mathcal{G}}(y)) > \tau) CE(\mathbf{p}_\varphi^{\mathcal{G}}(y), \hat{p}_\varphi^{\mathcal{G}}(y)) \tag{2}$$

where CE(.,.) is the cross-entropy function, $\mathcal{B} = \{\mathcal{G}_i\}_{i=1}^{|\mathcal{B}|}$ is a sample batch, and $\tau$ is a confidence threshold. $\tau$ excludes low-certainty predictions (samples less aligned with the source data distribution) and can be fixed or class-dynamic (see Appendix A.5.3)

### 3.2 Prompt Regularization

**Diversity.** Due to the class imbalance, only reducing the consistency loss may cause biased predictions and trivial solutions such that every sample is assigned to the same class to reduce the overall entropy. To mitigate this, inspired by Liang et al. (2020a), we regularize the model to maximize the entropy of the scores' expected value over a batch, and encourage diverse predictions.

$$\mathcal{L}_{div} = -H(\hat{\mathbf{q}}) = \mathbf{1}^\top (\hat{\mathbf{q}} \odot \log \hat{\mathbf{q}}); \; \hat{\mathbf{q}} = \frac{1}{|\mathcal{B}|} \sum_{\mathcal{G} \in \mathcal{B}} \hat{p}_\varphi^{\mathcal{G}}(y) \tag{3}$$

Here $H(.)$ is the entropy function, and $\odot$ is the Hadamard product. Employing consistency regularization with an adjusted confidence threshold ($\tau$) and integrating a diversity loss ($\mathcal{L}_{div}$) to prevent class collapse helps our framework address pseudo-label dependency and potential calibration risks.

**Domain Adaptation.**While the prompting function $f$ minimizes the discrepancy of predictions for the same sample, it may also create OOD prompted graphs. However, even without access to the source data samples, the knowledge learned from these samples is preserved in the frozen parameters $\theta_\varphi$. We utilize this information to mitigate the OOD issue. To achieve this, we train an adversarial discriminator $d(.; \theta_d)$—e.g. a simple feedforward network with trainable parameters $\theta_d$—to distinguish a prompted graph $\mathcal{G}_p$ from a non-prompted augmented graph $\mathcal{G}_w$. Formally, we optimize the discriminator as follows:

$$\theta_d^\star = \arg\min_{\theta_d} -\frac{1}{2|\mathcal{B}|} \sum_{\mathcal{G} \in \mathcal{B}} [\log \sigma(d(z_a^{\mathcal{G}}; \theta_d)) + \log(1 - \sigma(d(z_p^{\mathcal{G}}, \theta_d)))] \tag{4}$$

where $\sigma(.)$ is the sigmoid function. We normalize the sum by $\frac{1}{2|\mathcal{B}|}$ since every graph has two samples. Note that, $\mathcal{L}_d$ is only used to optimize the discriminator and does not appear in the final objective. Nevertheless, we regularize $f$ with the following objective to make $g$'s representations for prompted graphs closer to the non-prompted augmented graphs.

$$\mathcal{L}_{adv} = -\frac{1}{|\mathcal{B}|} \sum_{\mathcal{G} \in \mathcal{B}} \log \sigma(d(z_p^{\mathcal{G}}; \theta_d^\star)) \tag{5}$$

### 3.3 Final Objective & Complexity Analysis

Our unsupervised objective approach involves three parts. Eq. 2 encourages consistency across GNN predictions to handle distribution shift and exploit the GNN's learned knowledge from source data. Eq. 3 and Eq. 5 handle class imbalance and avoid generating OOD prompted graph respectively. The final objective to optimize $\theta_f$ becomes:

$$\theta_f^\star = \arg\min_{\theta_f} \mathcal{L}; \qquad \mathcal{L} = \mathcal{L}_c + \lambda_1 \mathcal{L}_{div} + \lambda_2 \mathcal{L}_{adv} \tag{6}$$

where $\lambda_1, \lambda_2$ are hyper-parameters. We bring empirical evidence supporting the logic behind adding each of the regularization objectives terms in the Appendix A.7.6.

During inference, the augmentation step is skipped, allowing the prompting module to produce a prompted graph directly from an input graph to align it with the pre-trained model's knowledge. This

Table 1: Graph classification results on target datasets (for GCN and GAT base models) show our unsupervised UGPROMPT largely outperforming competitors that use 25% labeled data.

| Base GNN | Method | %Label | ENZYMES | | PROTEINS | | DHFR | | BBBP | | BACE | |
|---|---|---|---|---|---|---|---|---|---|---|---|---|
| | | | F1 | IMP | F1 | IMP | F1 | IMP | F1 | IMP | F1 | IMP |
| GCN | BaseModel | 0 | 47.7±5.7 | - | 51.8±7.0 | - | 75.5±6.3 | - | 87.3±1.2 | - | 58.5±3.3 | - |
| | Fine-Tuning | 25 | 46.4±0.1 | -2.7 | 47.5±0.7 | -8.3 | 76.8±0.1 | 1.7 | **88.3**±1.2 | **1.1** | 64.0±0.7 | 1.1 |
| | GraphPrompt | | 38.1±1.4 | -20.1 | 50.8±1.4 | -1.9 | 71.7±1.1 | -5.0 | 81.9±1.2 | -6.2 | 64.3±0.7 | 9.9 |
| | GraphPrompt+ | | 23.5±2.5 | -50.7 | 44.7±5.1 | -13.7 | 64.9±6.2 | -14.0 | 82.0±1.2 | -6.1 | 61.0±3.1 | 8.4 |
| | All-In-One | | 45.8±1.9 | -4.0 | 38.1±13.4 | -26.4 | **79.1**±0.6 | **4.6** | 85.7±1.2 | -1.8 | 52.5±6.1 | -10.3 |
| | GPF-Plus | | 48.3±1.8 | 1.3 | 53.8±2.6 | 3.9 | 76.9±0.3 | 1.9 | 88.0±1.2 | 0.8 | 63.4±1.2 | 8.4 |
| | UGPROMPT | **0** | **49.1**±0.6 | **2.9** | **56.0**±1.5 | **8.1** | 77.0±2.4 | 2.0 | **88.3**±0.2 | **1.1** | **64.6**±1.9 | **10.4** |
| GAT | BaseModel | 0 | 44.1±6.4 | - | 51.5±8.1 | - | 77.3±3.5 | - | 87.7±1.2 | - | 46.4±1.2 | - |
| | Fine-Tuning | 25 | 42.9±0.0 | -2.7 | 50.2±0.8 | -2.5 | 76.5±0.0 | -1.0 | **88.4**±0.1 | **0.8** | 46.4±0.7 | -2.7 |
| | GraphPrompt | | 29.3±1.0 | -33.6 | 49.5±1.1 | -3.9 | 72.8±0.8 | -5.8 | 83.4±0.3 | -4.9 | 57.9±0.5 | 0.0 |
| | GraphPrompt+ | | 25.7±4.6 | -41.7 | 48.7±7.7 | -5.4 | 57.2±9.1 | -26.0 | 82.4±2.0 | -6.0 | 64.2±3.7 | 10.9 |
| | All-In-One | | 39.5±2.5 | -10.4 | 31.5±14.8 | -38.8 | 76.0±2.0 | -1.7 | 86.5±0.4 | -1.4 | 57.9±3.9 | -9.8 |
| | GPF-Plus | | 42.9±2.0 | -2.7 | 54.9±1.9 | 3.7 | 77.3±0.9 | 0.0 | 88.3±0.3 | 0.7 | 65.8±0.9 | 13.6 |
| | UGPROMPT | **0** | **45.9**±2.2 | **4.1** | **56.4**±2.0 | **9.5** | **78.2**±0.9 | **1.2** | 87.8±0.2 | 0.1 | **66.1**±0.2 | **14.2** |

prompted graph is passed to the pre-trained GNN for prediction. The pseudocode of UGPROMPT for both the training and inference are presented in Algorithms 1 and 2 respectively (see the Appendix).

The time complexity of a regular GNN (e.g. GCN), is $O(NLd^2 + L|E|d)$, where $N$,$E$, $L$, and $d$ are the number of nodes, edges, GNN layers, and the dimensionality of node embeddings respectively. A common graph augmentation algorithm like feature masking requires $O(Nd)$ operations. The complexity of the prompting method used in our experiments is $NdN^*$, where $N^*$ is the number of trainable prompting vectors. Thus, the overall complexity is $O(NLd^2 + L|E|d + NdN^*)$. We compare our training and test times against the baselines in Appendix A.7.9 and show that UGPROMPT is more efficient than average at the test time.

## 4 EXPERIMENTS

**Datasets and Code.** We experiment on six standard datasets for graph and node classification. We use ENZYMES Schomburg et al. (2004), PROTEINS Borgwardt et al. (2005), DHFR Sutherland et al. (2003), BBBP and BACE Wu et al. (2017) datasets for graph classification, which have continuous or discrete features. For node classification, we use Cora, CiteSeer, PubMed Yang et al. (2016), Flickr Zeng et al. (2020), Cornell, Texas, Wisconsin Pei et al. (2020). Please find more details in Appendix A.5.1. The code is available at `https://anonymous.4open.science/r/UGPrompt-6C3E`.

*Distribution Shift in Datasets.* Our problem definition (UGPP) requires evaluating a pre-trained GNN on target datasets that exhibit a covariate shift from the source data. To implement this, our main experiments induce shifts based on fundamental graph properties. For graph classification, we generate datasets with varying edge homophily ratios Zhu et al. (2020), a property known to intrinsically affect GNN information aggregation Gilmer et al. (2017). For node classification, we use PageRank Bazhenov et al. (2023) to create a popularity-based shift, which provides a challenging evaluation scenario Bazhenov et al. (2023). Further details on the generation of these distributions are in Appendix A.5.2, and additional experiments on other shifts (e.g., graph density, clustering coefficient) are in Appendix A.7.2.

**Evaluation Setting.** All datasets are split in half to create source and target sets with shifted distributions. We train a base GNN on the source set and evaluate it on the target set. Since baseline prompting methods rely on supervised training, we allow only the baselines to access labeled data for training in four setups of 25%, 50%, 75%, and 100% (full supervision). Please find experiments on 50%, 75% and 100% labeled data in Appendix A.7.12. We report F1-score, and F1-score improvement, referred to as IMP, compared to the BaseModel baseline.

Table 2: Node classification results on target datasets for GCN as the base model. Compared to baselines given 25% of labeled data, UGPROMPT generally achieves better results without labels.

| Base GNN | Method | %Label | Cora | | CiteSeer | | PubMed | | Flickr | | Cornell | | Texas | | Wisconsin | |
|---|---|---|---|---|---|---|---|---|---|---|---|---|---|---|---|---|
| | | | F1 | IMP | F1 | IMP | F1 | IMP | F1 | IMP | F1 | IMP | F1 | IMP | F1 | IMP |
| GCN | BaseModel | 0 | 53.8$^{\pm 2.4}$ | - | 44.1$^{\pm 1.5}$ | - | 57.1$^{\pm 0.8}$ | - | 16.5$^{\pm 0.4}$ | - | 19.1$^{\pm 6.2}$ | - | 23.6$^{\pm 10.3}$ | - | 25.2$^{\pm 10.2}$ | - |
| | Fine-Tuning | 25 | 51.7$^{\pm 0.5}$ | -3.9 | 40.0$^{\pm 0.3}$ | -9.3 | 54.3$^{\pm 3.4}$ | -4.9 | 10.4$^{\pm 0.1}$ | -37.0 | 19.1$^{\pm 0.0}$ | 0.0 | 26.4$^{\pm 0.0}$ | 11.9 | 27.1$^{\pm 0.1}$ | 7.5 |
| | GPPT | | 47.8$^{\pm 3.5}$ | -11.2 | 38.4$^{\pm 0.5}$ | -12.9 | 51.6$^{\pm 4.8}$ | -9.6 | 13.5$^{\pm 0.5}$ | -18.2 | 15.1$^{\pm 3.0}$ | -20.9 | 25.6$^{\pm 8.6}$ | 8.5 | 23.4$^{\pm 0.1}$ | -7.1 |
| | GraphPrompt | | 53.8$^{\pm 0.4}$ | 0.0 | 41.6$^{\pm 0.3}$ | -5.7 | 56.9$^{\pm 0.1}$ | -0.4 | 13.0$^{\pm 0.1}$ | -21.2 | 10.9$^{\pm 1.4}$ | -42.9 | 4.8$^{\pm 0.4}$ | -79.7 | 10.5$^{\pm 0.1}$ | -58.3 |
| | GraphPrompt+ | | 49.8$^{\pm 0.3}$ | -7.4 | 39.9$^{\pm 0.3}$ | -9.5 | **62.0**$^{\pm 0.4}$ | **8.6** | 14.8$^{\pm 0.6}$ | -10.3 | 11.5$^{\pm 2.1}$ | -39.8 | 4.8$^{\pm 0.3}$ | -79.9 | 12.0$^{\pm 0.1}$ | -52.3 |
| | All-In-One | | 50.5$^{\pm 1.1}$ | -6.1 | 38.3$^{\pm 1.0}$ | -13.2 | 42.1$^{\pm 0.9}$ | -26.3 | 13.8$^{\pm 0.3}$ | -16.4 | 13.0$^{\pm 0.8}$ | -31.9 | 21.7$^{\pm 1.6}$ | -8.1 | 21.4$^{\pm 0.1}$ | -15.1 |
| | GPF-Plus | | 56.5$^{\pm 0.6}$ | 5.0 | 45.6$^{\pm 0.6}$ | 3.4 | 59.1$^{\pm 0.4}$ | 3.5 | 13.3$^{\pm 0.3}$ | -19.4 | 22.0$^{\pm 0.5}$ | 15.2 | 25.2$^{\pm 1.4}$ | 6.8 | 26.7$^{\pm 0.1}$ | 6.0 |
| | UGPROMPT | **0** | **57.3**$^{\pm 0.4}$ | **6.5** | **45.7**$^{\pm 0.4}$ | **3.6** | 61.2$^{\pm 0.3}$ | 7.2 | **17.5**$^{\pm 0.4}$ | **6.1** | **23.2** $^{\pm 0.5}$ | **21.5** | **26.8**$^{\pm 0.8}$ | **13.6** | **28.0**$^{\pm 0.1}$ | **11.1** |
| GAT | BaseModel | 0 | 47.7$^{\pm 1.3}$ | - | 41.2$^{\pm 2.4}$ | - | 60.0$^{\pm 1.1}$ | - | 17.0$^{\pm 0.2}$ | - | 18.6$^{\pm 0.2}$ | - | 28.1$^{\pm 0.2}$ | - | 19.9$^{\pm 6.9}$ | - |
| | Fine-Tuning | 25 | 43.5$^{\pm 0.6}$ | -8.8 | 38.8$^{\pm 0.3}$ | -5.8 | 55.6$^{\pm 2.7}$ | -7.3 | 10.9$^{\pm 0.2}$ | -35.9 | 18.2$^{\pm 0.0}$ | -2.2 | 21.2$^{\pm 0.0}$ | -24.6 | 21.8$^{\pm 0.0}$ | 9.5 |
| | GPPT | | 31.5$^{\pm 3.9}$ | -34.0 | 34.3$^{\pm 1.8}$ | -16.7 | 51.7$^{\pm 4.6}$ | -13.8 | 12.9$^{\pm 0.1}$ | -24.1 | 17.2$^{\pm 4.5}$ | -7.5 | 28.2$^{\pm 5.5}$ | 0.4 | 21.5$^{\pm 4.1}$ | 8.0 |
| | GraphPrompt | | 44.2$^{\pm 0.6}$ | -7.3 | 39.2$^{\pm 0.4}$ | -4.9 | 60.1$^{\pm 0.1}$ | 0.2 | 13.4$^{\pm 0.3}$ | -21.1 | 14.3$^{\pm 1.3}$ | -23.1 | 1.4$^{\pm 0.0}$ | -95.0 | 15.4$^{\pm 1.5}$ | -22.6 |
| | GraphPrompt+ | | 41.2$^{\pm 0.9}$ | -13.6 | 37.8$^{\pm 0.7}$ | -8.3 | **64.0**$^{\pm 1.1}$ | **6.7** | 17.5$^{\pm 0.6}$ | 2.9 | 13.5$^{\pm 2.0}$ | -27.4 | 1.4$^{\pm 0.0}$ | -95.0 | 17.1$^{\pm 2.4}$ | -14.1 |
| | All-In-One | | 34.3$^{\pm 2.1}$ | -28.1 | 27.6$^{\pm 1.4}$ | -33.0 | 22.7$^{\pm 3.2}$ | -62.2 | 13.3$^{\pm 0.2}$ | -21.8 | 13.5$^{\pm 0.2}$ | -27.4 | 21.2$^{\pm 0.7}$ | -24.6 | 16.9$^{\pm 0.9}$ | -15.1 |
| | GPF-Plus | | 47.6$^{\pm 1.5}$ | -0.2 | 42.1$^{\pm 0.6}$ | 2.2 | 60.1$^{\pm 0.3}$ | 0.2 | 13.8$^{\pm 0.2}$ | -18.8 | 17.9$^{\pm 1.1}$ | -3.8 | **30.4**$^{\pm 0.7}$ | **8.2** | 21.7$^{\pm 1.2}$ | 9.0 |
| | UGPROMPT | **0** | **48.8**$^{\pm 0.9}$ | **2.3** | **42.3**$^{\pm 0.5}$ | **2.7** | 60.2$^{\pm 0.1}$ | 0.3 | **17.6**$^{\pm 0.3}$ | **3.5** | **21.8**$^{\pm 1.5}$ | **17.2** | 29.5$^{\pm 1.0}$ | 5.0 | **22.2**$^{\pm 1.1}$ | **11.6** |

**Baselines.** We consider several types of baselines.
*(1) BaseModel.* The base GNN without prompting and fine-tuning, which is expected to be outperformed by prompting methods. We use GCN Kipf & Welling (2017) and GAT Veličković et al. (2018) as the base GNN. More experiments with recent advanced GNNs are in Appendix A.7.3.
*(2) Fine-Tuning.* The base GNN model when we fix its encoder and just fine-tune its projection head. The goal is to verify the claim that fine-tuning on new dataset with labels does not necessarily improve performance Sun et al. (2022); Fang et al. (2023); Sun et al. (2023).
*(3)* GNN *Prompting Methods.* Our work is the first attempt for graph prompting without labels and updating the base GNN's parameters. Thus, we compare with all the SOTA GNN prompting methods used in the recent benchmark Zi et al. (2024), namely All-In-One Sun et al. (2023) and GPF-Plus Fang et al. (2023), GraphPrompt Liu et al. (2023b), GraphPrompt+ Yu et al. (2024a), and GPPT Sun et al. (2022). We do not allow these methods to update the GNN's parameters and only their prompting modules are supposed to be learned on the target dataset. We use the codebases from the corresponding papers.

### 4.1 RESULTS ON GRAPH CLASSIFICATION

For graph classification, 50% of graphs are randomly sampled as the source dataset, with graphs of higher homophily having a greater chance of selection; the remaining 50% form the target dataset. Please see experiments with graph density distribution shift in Table 11 (see the Appendix). The base GNN is trained on the source dataset. We repeat the experiments for two base GNNs (GCN and GAT) to show how the models generalize over different architectures. Note that GPPT is limited to node classification so we exclude it from this experiment.

Table 1 presents graph classification results, where baselines use 25% labeled data, while our method, UGPROMPT, uses 0%. Two key observations highlight UGPROMPT's contribution: first, it consistently surpasses the BaseModel, validating it as a reliable, non-detrimental prompting method. Second, and *most notably,* UGPROMPT*'s use of no labels offers broad applicability to diverse unlabeled datasets, marking a step towards graph foundation models.* Interestingly, evaluations with UGPP setting reveal that baselines often fail to improve performance and sometimes make it worse. Most of the graph prompting methods, except for GPF-Plus, perform poorly with both GNN architectures. Although GPF-Plus has the same prompting function as UGPROMPT's, it struggles with adapting to distribution shifts. Conversely, UGPROMPT leverages source data knowledge and generates pseudo-labels from highly confident predictions, learning effectively from samples that closely match the source distribution. This ensures consistent improvement across all cases.

### 4.2 RESULTS ON NODE CLASSIFICATION

First, we compute PageRank (PR) for all nodes of each dataset. We sample 50% of nodes for the source dataset according to the normalized PR such that graphs with higher PR are more likely

Table 3: UGPROMPT performance on under different augmentation rates $p_s$ for the prompted augmented graph. Higher values of $p_s$ provide more variation in masked feature groups and generally helping with capturing distribution shifts better.

| $p_s$ | ENZYMES | | PROTEINS | | DHFR | | Cora | | CiteSeer | | PubMed | |
|---|---|---|---|---|---|---|---|---|---|---|---|---|
| | F1 | IMP | F1 | IMP | F1 | IMP | F1 | IMP | F1 | IMP | F1 | IMP |
| 0.0 | 47.7 | - | 55.7 | - | 76.8 | - | 56.3 | - | 44.9 | - | 57.2 | - |
| 0.1 | **49.1** | **2.9** | 55.7 | 0.0 | **77.0** | **0.3** | 56.7 | 0.7 | 44.9 | 0.0 | 58.6 | 2.4 |
| 0.2 | 48.9 | 2.5 | 55.9 | 0.4 | 76.8 | 0.0 | 56.8 | 0.9 | 45.0 | 0.2 | 59.7 | 4.4 |
| 0.3 | 48.1 | 0.8 | **56.0** | **0.5** | 76.2 | -0.8 | 57.1 | 1.4 | 45.2 | 0.7 | 60.4 | 5.6 |
| 0.4 | 46.9 | -1.7 | 55.6 | -0.2 | 75.7 | -1.4 | **57.3** | **1.8** | **45.7** | **1.8** | **61.2** | **7.0** |

included in the source dataset. The rest are assigned to the target dataset. A 2-hop neighborhood of each node is extracted as a subgraph for task unification to graph classification and it inherits the main node's label. More experiments with distribution shift of type clustering coefficient are provided in Table 12 (see the Appendix).

Node classification results are in Table 2. UGPROMPT outperforms on all datasets except PubMed (where it is second-best) and, *notably, uses no labeled data, unlike the baselines.* Additionally, the GNN's performance degrades on target data across all datasets after fine-tuning its projection head (the Fine-Tuning baseline) with 25% of labels. This verifies that fine-tuning a model on a small-sized labeled dataset may introduce noisy information when the downstream data distribution does not align with the model's learned knowledge Bousquet et al. (2004); Shalev-Shwartz & Ben-David (2014); Brown et al. (2020). We also verify UGPROMPT maintains high performance on the source domain, and does not impose forgetting the learned knowledge, unlike the other baselines; please find the experiments in Appendix A.7.7. An important advantage of an unsupervised method—such as ours—is that it allows utilizing large-scale unlabeled datasets. It is important to emphasize that UGPROMPT achieves the best results on Flickr, the largest dataset, and second best with high margins from other baselines on PubMed, the second largest dataset, which indicates UGPROMPT can perform well on large data.

## 4.3 ABLATION STUDY

### 4.3.1 THE EFFECT OF REGULARIZATION

To evaluate the regularization effect, UGPROMPT is trained in four scenarios: (1) without regularization ("w/o"), (2) with only domain adaptation regularization ("domain"), (3) with only diversity regularization ("diversity"), and (4) with both regularizations ("domain + diversity"). Settings (2), (3), and (4) are compared to (1), with Figure 2 showing IMP improvements. If a regularization term fails to enhance the model, IMP is set to zero meaning it can be neutralized (setting $\lambda_1$ or $\lambda_2$ to zero) in Equation 6. Results show that both regularization factors have positive effects across the majority of datasets; however, their combination is not always superior to individual application. Domain adaptation regularization is beneficial across all graph classification datasets. We conjecture that the distributions of node classification datasets are more likely to be densely populated, whereas graph datasets often exhibit scattered hollow spaces in the latent space between classes, increasing the likelihood of generating OOD-prompted graphs. Therefore, domain adaptation regularization would be more beneficial. Moreover, a key finding of this experiment is the importance of adding diversity regularization. More specifically, when we have severe class imbalance for example in PROTEINS, Cora, and CiteSeer, "diversity" empowers the base GNN significantly, which supports our claims. Appendix A.7.6 provides more discussion on the effect of these objectives.

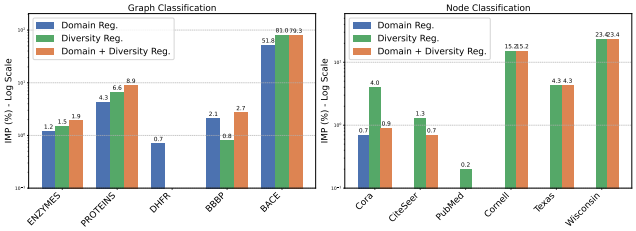


Figure 2: The effect of regularization objectives on UGPROMPT with GCN as the base model.

Table 4: Evaluation of UGPROMPT 's performance in a few-shot setting using GCN as the base GNN under homophily and PR distribution shifts. Results indicate considerable gains with labeled data, particularly in node classification tasks.

| Method | %Label | ENZYMES | | PROTEINS | | DHFR | | Cora | | CiteSeer | | PubMed | |
|---|---|---|---|---|---|---|---|---|---|---|---|---|---|
| | | F1 | IMP | F1 | IMP | F1 | IMP | F1 | IMP | F1 | IMP | F1 | IMP |
| BaseModel | | 47.7 | - | 51.8 | - | 75.5 | - | 53.8 | - | 44.1 | - | 57.1 | - |
| UGPROMPT (ours) | 25 | **49.1** | **2.9** | **56.2** | **8.5** | **77.2** | **2.3** | **58.2** | **8.2** | **47.0** | **6.6** | **63.5** | **11.2** |
| | 10 | 49.0 | 2.7 | 56.1 | 8.3 | 77.0 | 2.0 | 57.6 | 7.1 | 46.2 | 4.8 | 62.1 | 8.8 |
| | 5 | **49.1** | **2.9** | 56.1 | 8.3 | 77.1 | 2.1 | 57.5 | 6.9 | 46.0 | 4.3 | 62.1 | 8.8 |
| | 0 | **49.1** | **2.9** | 56.0 | 8.1 | 77.0 | 2.0 | 57.3 | 6.5 | 45.7 | 3.6 | 61.2 | 7.2 |

Table 5: Scaling with homophily shift across four target sets. UGPROMPT is better in most cases.

| Target set | Method | ENZYMES | PROTEINS | DHFR | BACE | Cora | CiteSeer |
|---|---|---|---|---|---|---|---|
| **Set 1** | GPF-Plus | -3.6 | 11.5 | -3.2 | 20.7 | -1.8 | 0.2 |
| | **UGPrompt** | **0.9** | **19.6** | **-0.6** | **40.1** | **0.7** | **2.0** |
| **Set 2** | GPF-Plus | -5.4 | 57.6 | -1.9 | 106.1 | 2.4 | 0.2 |
| | **UGPrompt** | **1.0** | **62.0** | **2.0** | **155.6** | **2.6** | **0.7** |
| **Set 3** | GPF-Plus | **27.1** | 85.7 | **10.2** | 108.8 | **2.2** | **2.1** |
| | **UGPrompt** | 3.0 | **89.2** | 7.3 | **124.7** | 0.2 | 0.5 |
| **Set 4** | GPF-Plus | -7.8 | 44.4 | **3.7** | 97.3 | -2.6 | 1.3 |
| | **UGPrompt** | **1.9** | **46.4** | 2.7 | **113.7** | **3.5** | **1.9** |

#### 4.3.2 THE EFFECT OF AUGMENTATION

We mask node features in weakly augmented graphs ($\mathcal{G}_w$) for pseudo-labeling with probability $p_w$ and in strongly augmented graphs $\mathcal{G}_s$ for prompting with probability $p_s$. Since $\mathcal{G}_s$ resembles a distribution shift from $\mathcal{G}_w$, a higher $p_s$ allows learning from distribution shifts across more feature groups offering potentially more robustness. Here, we fix $p_w = 0.1$ and evaluate the impact of varying $p_s$. The IMP for all $p_s$ values is compared to no augmentation $p_s = 0$. The results in Table 3 support our intuition that augmenting, confidence pseudo-labeling, and consistency training are advantageous. Higher $p_s$ yields better performance, over PROTEINS, Cora, CireSeer, and PubMed because augmentation by feature masking—replacing a group of feature values with 0.0—is semantically more aligned with the discrete and binary features of these datasets; however, for ENZYMES and DHFR with continuous features, this augmentation is not as effective and higher values of $p_s$ may be detrimental and cause learning from noise. Additional experiments on evaluating the effect of augmentation type (e.g. modifying graph structure) are in Appendix A.7.11. Besides, we show the versatility and generalization of our framework in Appendix A.7.10 using All-In-One's prompting function as a choice of function $f$ (see Section 3.1).

#### 4.3.3 THE EFFECT OF HOMOPHILY SHIFT

To evaluate how performance scales with the increase in covariate shift (or difficulty), we extend our experiment by constructing explicit degrees of shift. Instead of a random 50–50 split (as in the original setting), we sort all samples by homophily (for the graph classification dataset) and PageRank (for node classification datasets). The top 50% (highest homophily) are used as the source dataset. The remaining 50% are divided into four target sets with increasing difficulty (amount of covariate shift with respect to source set): (i) Set 1: 50–67.5 (closest to source), (ii) Set 2: 67.5–75, (iii) Set 3: 75–87.5, and (iv) Set 4: 87.5–100 (lowest homophily). Table 5 shows the results. UGPROMPT maintains strong gains on the easier shifts (Sets 1 & 2) and continues to deliver improvements even under severe distribution shift (Sets 3 & 4). In contrast, GPF-Plus is worse and frequently induces negative transfer (negative IMP%).

### 4.4 FEW-SHOT LEARNING FOR UGPROMPT

UGPROMPT is an unsupervised GNN prompting method. However, it can potentially utilize labeled data efficiently when it is available. Assuming every batch $\mathcal{B}$ is composed of a set of labeled samples $S_l$ and unlabeled samples $S_u$ s.t. $\mathcal{B} = S_l \cup S_u$, we can replace $\mathcal{L}_c$ in Equation 2 by $\mathcal{L}_c = \frac{1}{|\mathcal{B}|}(\mathcal{L}_l + \lambda_3 \mathcal{L}_u)$ in which $\mathcal{L}_l = \sum_{\mathcal{G} \in S_l} CE(y^{\mathcal{G}}, \hat{p}^{\mathcal{G}}_{\varphi}(y))$ is the supervised objective term and $\mathcal{L}_u = \sum_{\mathcal{G} \in \mathcal{B}} \mathbb{1}(\max(\tilde{p}^{\mathcal{G}}_{\varphi}(y)) \geq \tau) CE(\mathbf{p}^{\mathcal{G}}_{\varphi}(y), \hat{p}^{\mathcal{G}}_{\varphi}(y))$ is the unsupervised term.

Table 7: Cross-dataset transfer results. All values are IMP%. UGPROMPT consistently delivers positive transfer. C, T and W denote is Cornell, Texas, and Wisconsin respectively.

| | C→T | C→W | T→C | T→W | W→C | W→T |
|---|---|---|---|---|---|---|
| GPF-Plus | -3.4 | 81.1 | -5.0 | 61.9 | 33.0 | 209.8 |
| **UGPrompt** | 11.1 | 10.4 | 6.2 | 1.2 | 41.5 | 123.5 |

Here we evaluate UGPROMPT in a few-shot setting. Table 4 presents the results using GCN as the base GNN under homophily and PR distribution shifts. UGPROMPT significantly performs better when labels are provided. For node classification datasets, IMP of the 25% labels setting is notably more than that of the unsupervised case (0% labels), while improvements on PROTEINS and DHFR are smaller. Meanwhile, performance on ENZYMES remains comparable in the absence of labels, likely due to a significant covariate shift, which makes learning from highly heterophilic data challenging even with labels. The key takeaway emerges by comparing Table 4 with Tables 1 and 2, showing that with 25% of labeled data, UGPROMPT outperforms all baselines on most datasets except DHFR. Notably, its superiority is also evident in the 0% label setting.

### 4.5 ROBUSTNESS UNDER REAL-WORLD SHIFTS

To test robustness beyond simulated covariate shift, we design two experiments. We use the Cornell, Texas, and Wisconsin datasets, which share the same feature dimensionality and number of classes. In the first experiment, we evaluate a setting where the source and target datasets have different class distributions. For each of the datasets, the base GNN is pre-trained on classes $\{0, 1, 2\}$—each dataset has 5 classes. Then the base is frozen, prompted, and evaluated on classes $\{2, 3, 4\}$ (reindexed to $\{0, 1, 2\}$). Table 6 summarizes the findings. The BaseModel collapses under this strong semantic/label shift, whereas UGPROMPT recovers substantial performance across all datasets, outperforming GPF-Plus (the baseline), which occasionally leads to negative transfer.

Table 6: Evaluation under label distribution shift with disjoint labels for source and target datasets. Upper panel: the BaseModel's F1-score on the source and target domains (showing the severity of the shift). Lower panel: prompting methods' improvements (IMP %) on the target domain.

| **Method** | **Cornell** | **Texas** | **Wisconsin** |
|---|---|---|---|
| **BaseModel Performance (F1-score)** | | | |
| Source | 46.7 | 79.8 | 60.1 |
| Target | 15.3 | 13.1 | 13.9 |
| **Target Domain Improvement (IMP%)** | | | |
| GPF-Plus | 30.1 | -1.5 | 5.4 |
| **UGPrompt** | **36.6** | **9.9** | **28.1** |

Our second experiment is designed to evaluate robustness to real-world covariate shift. We consider a more extreme scenario compared to the simulated covariate shift as discussed before. This setting is standard (particularly in transfer learning) and more challenging. Here, we train the base GNN on a source dataset, such as Cornell, and then prompt and evaluate it on another dataset, such as Texas, which is denoted as Cornell → Texas. Results are shown in Table 7. UGPROMPT consistently delivers positive transfer, whereas GPF-Plus potentially produces negative transfer. This demonstrates UGPROMPT's robustness even under severe shifts.

## 5 CONCLUSIONS

In conclusion, we have introduced UGPROMPT,
a novel unsupervised prompting framework for GNNs that overcomes the limitations of existing prompting methods, particularly in scenarios where labeled data is unavailable. UGPROMPT eliminates the need for updating the base GNN's parameters on new downstream tasks. UGPROMPT also enhances the generalization of the base pre-trained GNNs without supervision. Experimental results over various datasets validate the effectiveness of UGPROMPT which outperforms the state-of-the-art prompting methods that rely on labeled data on both graph and node classification tasks in many settings.

*Limitations & Future Work.* Since we do not
involve training the projection head of the pre-trained GNN for the downstream tasks, UGPROMPT is unable to handle label distribution shift. Consequently, our framework is also unable to employ multi-task/meta learning unless we allow the projection head to be optimized—which necessitates labeled data. Another interesting future direction would be to design a method that selects high-quality pseudolabels in case of a severe covariate distribution shift.

## Reproducibility Statement

To ensure the reproducibility of our findings, we have made our code and experimental procedures fully accessible. All experiments were conducted over 50 iterations, comprising 10 dataset perturbations with 5 distinct model initializations each, to ensure robust results. In Appendix A.1, we provide a link to an anonymous repository containing the complete source code, environmental configurations, and the specific setups required to replicate our results across all datasets. Further details on our dataset selection, experimental design, and implementation are available in Appendix A.5.

## References

Philip Bachman, Ouais Alsharif, and Doina Precup. Learning with pseudo-ensembles. In *Proceedings of the 27th International Conference on Neural Information Processing Systems - Volume 2*, pp. 3365–3373, 2014.

Gleb Bazhenov, Denis Kuznedelev, Andrey Malinin, Artem Babenko, and Liudmila Prokhorenkova. Evaluating robustness and uncertainty of graph models under structural distributional shifts. In *Thirty-seventh Conference on Neural Information Processing Systems*, 2023.

Karsten M. Borgwardt, Cheng Soon Ong, Stefan Schönauer, S. V. N. Vishwanathan, Alex J. Smola, and Hans-Peter Kriegel. Protein function prediction via graph kernels. *Bioinformatics*, 21:i47–i56, 2005.

Olivier Bousquet, Stéphane Boucheron, and Gábor Lugosi. *Introduction to Statistical Learning Theory*, pp. 169–207. Springer Berlin Heidelberg, 2004.

Shaked Brody, Uri Alon, and Eran Yahav. How attentive are graph attention networks? In *International Conference on Learning Representations*, 2022.

Tom Brown, Benjamin Mann, Nick Ryder, Melanie Subbiah, Jared D Kaplan, Prafulla Dhariwal, Arvind Neelakantan, Pranav Shyam, Girish Sastry, Amanda Askell, Sandhini Agarwal, Ariel Herbert-Voss, Gretchen Krueger, Tom Henighan, Rewon Child, Aditya Ramesh, Daniel Ziegler, Jeffrey Wu, Clemens Winter, Chris Hesse, Mark Chen, Eric Sigler, Mateusz Litwin, Scott Gray, Benjamin Chess, Jack Clark, Christopher Berner, Sam McCandlish, Alec Radford, Ilya Sutskever, and Dario Amodei. Language models are few-shot learners. In H. Larochelle, M. Ranzato, R. Hadsell, M.F. Balcan, and H. Lin (eds.), *Advances in Neural Information Processing Systems*, volume 33, pp. 1877–1901, 2020.

Qin Chen, Liang Wang, Bo Zheng, and Guojie Song. Dagprompt: Pushing the limits of graph prompting with a distribution-aware graph prompt tuning approach. In *Proceedings of the ACM on Web Conference 2025*, WWW '25, pp. 4346–4358. Association for Computing Machinery, 2025. ISBN 9798400712746.

Ting Chen, Simon Kornblith, Mohammad Norouzi, and Geoffrey Hinton. A simple framework for contrastive learning of visual representations. In *Proceedings of the 37th International Conference on Machine Learning*, 2020.

Jacob Devlin, Ming-Wei Chang, Kenton Lee, and Kristina Toutanova. BERT: Pre-training of deep bidirectional transformers for language understanding. In *Proceedings of the 2019 Conference of the North American Chapter of the Association for Computational Linguistics: Human Language Technologies, Volume 1 (Long and Short Papers)*, pp. 4171–4186, 2019.

Mucong Ding, Kezhi Kong, Jiuhai Chen, John Kirchenbauer, Micah Goldblum, David Wipf, Furong Huang, and Tom Goldstein. A closer look at distribution shifts and out-of-distribution generalization on graphs. In *NeurIPS 2021 Workshop on Distribution Shifts: Connecting Methods and Applications*, 2021.

Shaohua Fan, Xiao Wang, Chuan Shi, Peng Cui, and Bai Wang. Generalizing graph neural networks on out-of-distribution graphs. *IEEE Transactions on Pattern Analysis and Machine Intelligence*, 46(1):322–337, 2024.

Taoran Fang, Yunchao Mercer Zhang, Yang Yang, Chunping Wang, and Lei CHEN. Universal prompt tuning for graph neural networks. In *Neural Information Processing Systems*, 2023.

Abolfazl Farahani, Sahar Voghoei, Khaled Rasheed, and Hamid R. Arabnia. A brief review of domain adaptation. In Robert Stahlbock, Gary M. Weiss, Mahmoud Abou-Nasr, Cheng-Ying Yang, Hamid R. Arabnia, and Leonidas Deligiannidis (eds.), *Advances in Data Science and Information Engineering*, pp. 877–894. Springer International Publishing, 2021.

Bahare Fatemi, Jonathan Halcrow, and Bryan Perozzi. Talk like a graph: Encoding graphs for large language models. In *The Twelfth International Conference on Learning Representations*, 2024.

Justin Gilmer, Samuel S. Schoenholz, Patrick F. Riley, Oriol Vinyals, and George E. Dahl. Neural message passing for quantum chemistry. In *Proceedings of the 34th International Conference on Machine Learning - Volume 70*, pp. 1263–1272, 2017.

Shurui Gui, Xiner Li, Limei Wang, and Shuiwang Ji. GOOD: A graph out-of-distribution benchmark. In *Thirty-sixth Conference on Neural Information Processing Systems Datasets and Benchmarks Track*, 2022.

Zeyu Han, Chao Gao, Jinyang Liu, Jeff Zhang, and Sai Qian Zhang. Parameter-efficient fine-tuning for large models: A comprehensive survey. *Transactions on Machine Learning Research*, 2024. ISSN 2835-8856.

Weihua Hu, Takeru Miyato, Seiya Tokui, Eiichi Matsumoto, and Masashi Sugiyama. Learning discrete representations via information maximizing self-augmented training. In *Proceedings of the 34th International Conference on Machine Learning - Volume 70*, pp. 1558–1567, 2017.

Weihua Hu, Matthias Fey, Marinka Zitnik, Yuxiao Dong, Hongyu Ren, Bowen Liu, Michele Catasta, and Jure Leskovec. Open graph benchmark: Datasets for machine learning on graphs. In *Advances in Neural Information Processing Systems*, volume 33, pp. 22118–22133, 2020.

Qian Huang, Hongyu Ren, Peng Chen, Gregor Kržmanc, Daniel Zeng, Percy Liang, and Jure Leskovec. Prodigy: Enabling in-context learning over graphs. *ArXiv*, abs/2305.12600, 2023.

Youngeun Kim, Donghyeon Cho, Kyeongtak Han, Priyadarshini Panda, and Sungeun Hong. Domain adaptation without source data. *IEEE Transactions on Artificial Intelligence*, 2:508–518, 2021.

Thomas N. Kipf and Max Welling. Semi-supervised classification with graph convolutional networks. In *International Conference on Learning Representations*, 2017.

Boris Knyazev, Graham W Taylor, and Mohamed Amer. Understanding attention and generalization in graph neural networks. In *Advances in Neural Information Processing Systems*, volume 32, 2019.

Takeshi Kojima, Shixiang (Shane) Gu, Machel Reid, Yutaka Matsuo, and Yusuke Iwasawa. Large language models are zero-shot reasoners. In *Advances in Neural Information Processing Systems*, volume 35, pp. 22199–22213, 2022.

Samuli Laine and Timo Aila. Temporal ensembling for semi-supervised learning. In *International Conference on Learning Representations*, 2017.

Dong-Hyun Lee. Pseudo-label : The simple and efficient semi-supervised learning method for deep neural networks. *ICML 2013 Workshop : Challenges in Representation Learning (WREPL)*, 2013.

Brian Lester, Rami Al-Rfou, and Noah Constant. The power of scale for parameter-efficient prompt tuning. In Marie-Francine Moens, Xuanjing Huang, Lucia Specia, and Scott Wen-tau Yih (eds.), *Proceedings of the 2021 Conference on Empirical Methods in Natural Language Processing*, pp. 3045–3059, 2021.

Haoyang Li, Ziwei Zhang, Xin Wang, and Wenwu Zhu. Learning invariant graph representations for out-of-distribution generalization. In Alice H. Oh, Alekh Agarwal, Danielle Belgrave, and Kyunghyun Cho (eds.), *Advances in Neural Information Processing Systems*, 2022. URL https://openreview.net/forum?id=acKK8MQe2xc.

Haoyang Li, Xin Wang, Ziwei Zhang, and Wenwu Zhu. Ood-gnn: Out-of-distribution generalized graph neural network. *IEEE Trans. on Knowl. and Data Eng.*, 35(7):7328–7340, 2023. ISSN 1041-4347.

Jingjing Li, Zhiqi Yu, Zhekai Du, Lei Zhu, and Heng Tao Shen. A comprehensive survey on source-free domain adaptation. *IEEE Transactions on Pattern Analysis and Machine Intelligence*, 46(8): 5743–5762, 2024.

Xiang Lisa Li and Percy Liang. Prefix-tuning: Optimizing continuous prompts for generation. In *Proceedings of the 59th Annual Meeting of the Association for Computational Linguistics and the 11th International Joint Conference on Natural Language Processing*, pp. 4582–4597, 2021.

Jian Liang, Dapeng Hu, and Jiashi Feng. Do we really need to access the source data? source hypothesis transfer for unsupervised domain adaptation. In *International Conference on Machine Learning (ICML)*, pp. 6028–6039, 2020a.

Jian Liang, Dapeng Hu, and Jiashi Feng. Do we really need to access the source data? source hypothesis transfer for unsupervised domain adaptation. In *International Conference on Machine Learning*, pp. 6028–6039, 2020b.

Derek Lim, Felix Matthew Hohne, Xiuyu Li, Sijia Linda Huang, Vaishnavi Gupta, Omkar Prasad Bhalerao, and Ser-Nam Lim. Large scale learning on non-homophilous graphs: New benchmarks and strong simple methods. In *Advances in Neural Information Processing Systems*, 2021.

Pengfei Liu, Weizhe Yuan, Jinlan Fu, Zhengbao Jiang, Hiroaki Hayashi, and Graham Neubig. Pre-train, prompt, and predict: A systematic survey of prompting methods in natural language processing. *ACM Comput. Surv.*, 55(9), 2023a. ISSN 0360-0300.

Zemin Liu, Xingtong Yu, Yuan Fang, and Xinming Zhang. Graphprompt: Unifying pre-training and downstream tasks for graph neural networks. In *Proceedings of the ACM Web Conference 2023*, pp. 417–428. Association for Computing Machinery, 2023b.

Haitao Mao, Zhikai Chen, Wenzhuo Tang, Jianan Zhao, Yao Ma, Tong Zhao, Neil Shah, Mikhail Galkin, and Jiliang Tang. Position: Graph foundation models are already here, 2024a.

Haitao Mao, Lun Du, Yujia Zheng, Qiang Fu, Zelin Li, Xu Chen, Shi Han, and Dongmei Zhang. Source free graph unsupervised domain adaptation. In *Proceedings of the 17th ACM International Conference on Web Search and Data Mining*, pp. 520–528, 2024b.

Swaroop Mishra, Daniel Khashabi, Chitta Baral, Yejin Choi, and Hannaneh Hajishirzi. Reframing instructional prompts to GPTk's language. In *Findings of the Association for Computational Linguistics: ACL 2022*, pp. 589–612, 2022.

Christopher Morris, Fabrizio Frasca, Nadav Dym, Haggai Maron, İsmail İlkan Ceylan, Ron Levie, Derek Lim, Michael Bronstein, Martin Grohe, and Stefanie Jegelka. Future directions in the theory of graph machine learning, 2024.

Adam Paszke, Sam Gross, Soumith Chintala, Gregory Chanan, Edward Yang, Zachary DeVito, Zeming Lin, Alban Desmaison, Luca Antiga, and Adam Lerer. Automatic differentiation in pytorch. 2017.

Hongbin Pei, Bingzhe Wei, Kevin Chen-Chuan Chang, Yu Lei, and Bo Yang. Geom-gcn: Geometric graph convolutional networks. In *International Conference on Learning Representations*, 2020.

Alec Radford and Karthik Narasimhan. Improving language understanding by generative pre-training. 2018.

Alec Radford, Jeff Wu, Rewon Child, David Luan, Dario Amodei, and Ilya Sutskever. Language models are unsupervised multitask learners. 2019.

Ladislav Rampasek, Mikhail Galkin, Vijay Prakash Dwivedi, Anh Tuan Luu, Guy Wolf, and Dominique Beaini. Recipe for a general, powerful, scalable graph transformer. In *Advances in Neural Information Processing Systems*, 2022.

Sebastian Ruder, Matthew E. Peters, Swabha Swayamdipta, and Thomas Wolf. Transfer learning in natural language processing. In *Proceedings of the 2019 Conference of the North American Chapter of the Association for Computational Linguistics: Tutorials*, pp. 15–18, 2019.

Mehdi Sajjadi, Mehran Javanmardi, and Tolga Tasdizen. Regularization with stochastic transformations and perturbations for deep semi-supervised learning. In *Proceedings of the 30th International Conference on Neural Information Processing Systems*, pp. 1171–1179, 2016.

Ida Schomburg, Antje Chang, Christian Ebeling, Marion Gremse, Christian Heldt, Gregor Huhn, and Dietmar Schomburg. Brenda, the enzyme database: updates and major new developments. *Nucleic Acids Research*, 32:D431–D433, 2004.

Shai Shalev-Shwartz and Shai Ben-David. *Understanding Machine Learning: From Theory to Algorithms*. Cambridge University Press, 2014.

Kihyuk Sohn, David Berthelot, Chun-Liang Li, Zizhao Zhang, Nicholas Carlini, Ekin D. Cubuk, Alex Kurakin, Han Zhang, and Colin Raffel. Fixmatch: simplifying semi-supervised learning with consistency and confidence. In *Proceedings of the 34th International Conference on Neural Information Processing Systems*, 2020.

Yongduo Sui, Qitian Wu, Jiancan Wu, Qing Cui, Longfei Li, Jun Zhou, Xiang Wang, and Xiangnan He. Unleashing the power of graph data augmentation on covariate distribution shift. In *Advances in Neural Information Processing Systems*, volume 36, pp. 18109–18131, 2023.

Mingchen Sun, Kaixiong Zhou, Xin He, Ying Wang, and Xin Wang. Gppt: Graph pre-training and prompt tuning to generalize graph neural networks. In *Proceedings of the 28th ACM SIGKDD Conference on Knowledge Discovery and Data Mining*, pp. 1717–1727. Association for Computing Machinery, 2022. doi: 10.1145/3534678.3539249.

Xiangguo Sun, Hong Cheng, Jia Li, Bo Liu, and Jihong Guan. All in one: Multi-task prompting for graph neural networks. In *ACM SIGKDD Conference on Knowledge Discovery and Data Mining*, pp. 2120–2131, 2023.

Jeffrey J. Sutherland, Lee A. O'Brien, and Donald F. Weaver. Spline-fitting with a genetic algorithm: A method for developing classification structure-activity relationships. *Journal of Chemical Information and Computer Sciences*, 43(6):1906–1915, 2003.

Aäron van den Oord, Yazhe Li, and Oriol Vinyals. Representation learning with contrastive predictive coding. *ArXiv*, abs/1807.03748, 2018.

Petar Veličković, Guillem Cucurull, Arantxa Casanova, Adriana Romero, Pietro Liò, and Yoshua Bengio. Graph attention networks. In *International Conference on Learning Representations*, 2018.

Yidong Wang, Hao Chen, Qiang Heng, Wenxin Hou, Yue Fan, Zhen Wu, Jindong Wang, Marios Savvides, Takahiro Shinozaki, Bhiksha Raj, Bernt Schiele, and Xing Xie. Freematch: Self-adaptive thresholding for semi-supervised learning. In *The Eleventh International Conference on Learning Representations*, 2023.

Jason Wei, Xuezhi Wang, Dale Schuurmans, Maarten Bosma, brian ichter, Fei Xia, Ed Chi, Quoc V Le, and Denny Zhou. Chain-of-thought prompting elicits reasoning in large language models. In *Advances in Neural Information Processing Systems*, volume 35, pp. 24824–24837. Curran Associates, Inc., 2022.

Yingxin Wu, Xiang Wang, An Zhang, Xiangnan He, and Tat-Seng Chua. Discovering invariant rationales for graph neural networks. In *International Conference on Learning Representations*, 2022.

Zhenqin Wu, Bharath Ramsundar, Evan N. Feinberg, Joseph Gomes, Caleb Geniesse, Aneesh S. Pappu, Karl Leswing, and Vijay S. Pande. Moleculenet: a benchmark for molecular machine learning. *Chemical Science*, 9:513 – 530, 2017.

Jun Xia, Lirong Wu, Jintao Chen, Bozhen Hu, and Stan Z. Li. Simgrace: A simple framework for graph contrastive learning without data augmentation. In *Proceedings of the ACM Web Conference 2022*, pp. 1070–1079, 2022.

Qizhe Xie, Eduard H. Hovy, Minh-Thang Luong, and Quoc V. Le. Self-training with noisy student improves imagenet classification. *Conference on Computer Vision and Pattern Recognition (CVPR)*, pp. 10684–10695, 2020.

Chengrun Yang, Xuezhi Wang, Yifeng Lu, Hanxiao Liu, Quoc V Le, Denny Zhou, and Xinyun Chen. Large language models as optimizers. In *The Twelfth International Conference on Learning Representations*, 2024a.

Jingkang Yang, Kaiyang Zhou, Yixuan Li, and Ziwei Liu. Generalized out-of-distribution detection: A survey. *Int. J. Comput. Vision*, 132(12):5635–5662, 2024b. ISSN 0920-5691.

Shiqi Yang, Yaxing Wang, Joost van de Weijer, Luis Herranz, and Shangling Jui. Generalized source-free domain adaptation. In *2021 IEEE/CVF International Conference on Computer Vision (ICCV)*, pp. 8958–8967, 2021.

Zhilin Yang, William W. Cohen, and Ruslan Salakhutdinov. Revisiting semi-supervised learning with graph embeddings. In *Proceedings of the 33rd International Conference on International Conference on Machine Learning - Volume 48*, pp. 40–48, 2016.

Zhitao Ying, Dylan Bourgeois, Jiaxuan You, Marinka Zitnik, and Jure Leskovec. Gnnexplainer: Generating explanations for graph neural networks. In *Advances in Neural Information Processing Systems*, volume 32, 2019.

Kaichao You, Mingsheng Long, Zhangjie Cao, Jianmin Wang, and Michael I. Jordan. Universal domain adaptation. In *Proceedings of the IEEE/CVF Conference on Computer Vision and Pattern Recognition (CVPR)*, 2019.

Yuning You, Tianlong Chen, Yongduo Sui, Ting Chen, Zhangyang Wang, and Yang Shen. Graph contrastive learning with augmentations. In *Advances in Neural Information Processing Systems*, volume 33, pp. 5812–5823, 2020.

Xingtong Yu, Zhenghao Liu, Yuan Fang, Zemin Liu, Sihong Chen, and Xinming Zhang. Generalized graph prompt: Toward a unification of pre-training and downstream tasks on graphs. *IEEE Transactions on Knowledge and Data Engineering*, 36(11):6237–6250, 2024a.

Xingtong Yu, Chang Zhou, Yuan Fang, and Xinming Zhang. Multigprompt for multi-task pre-training and prompting on graphs. In *Proceedings of the ACM Web Conference 2024*, pp. 515–526. Association for Computing Machinery, 2024b. ISBN 9798400701719.

Xingtong Yu, Zhenghao Liu, Xinming Zhang, and Yuan Fang. Node-time conditional prompt learning in dynamic graphs. In *The Thirteenth International Conference on Learning Representations*, 2025a.

Xingtong Yu, Jie Zhang, Yuan Fang, and Renhe Jiang. Non-homophilic graph pre-training and prompt learning. In *Proceedings of the 31st ACM SIGKDD Conference on Knowledge Discovery and Data Mining V.1*, KDD '25, pp. 1844–1854. Association for Computing Machinery, 2025b. ISBN 9798400712456.

H. Yuan, H. Yu, S. Gui, and S. Ji. Explainability in graph neural networks: A taxonomic survey. *IEEE Transactions on Pattern Analysis and Machine Intelligence*, 45(05):5782–5799, 2023.

Hanqing Zeng, Hongkuan Zhou, Ajitesh Srivastava, Rajgopal Kannan, and Viktor Prasanna. Graphsaint: Graph sampling based inductive learning method. In *International Conference on Learning Representations*, 2020.

Bowen Zhang, Yidong Wang, Wenxin Hou, HAO WU, Jindong Wang, Manabu Okumura, and Takahiro Shinozaki. Flexmatch: Boosting semi-supervised learning with curriculum pseudo labeling. In *Advances in Neural Information Processing Systems*, volume 34, pp. 18408–18419, 2021.

Zhen Zhang, Meihan Liu, Anhui Wang, Hongyang Chen, Zhao Li, Jiajun Bu, and Bingsheng He. Collaborate to adapt: Source-free graph domain adaptation via bi-directional adaptation. In *Proceedings of the ACM Web Conference 2024*, pp. 664–675, 2024.

Ziyi Zhang, Weikai Chen, Hui Cheng, Zhen Li, Siyuan Li, Liang Lin, and Guanbin Li. Divide and contrast: source-free domain adaptation via adaptive contrastive learning. In *Proceedings of the 36th International Conference on Neural Information Processing Systems*, NIPS '22, 2022. ISBN 9781713871088.

Haihong Zhao, Aochuan Chen, Xiangguo Sun, Hong Cheng, and Jia Li. All in one and one for all: A simple yet effective method towards cross-domain graph pretraining. In *Proceedings of the 30th ACM SIGKDD Conference on Knowledge Discovery and Data Mining*, KDD '24, pp. 4443–4454. Association for Computing Machinery, 2024. ISBN 9798400704901.

Hongling Zheng, Li Shen, Anke Tang, Yong Luo, Han Hu, Bo Du, Yonggang Wen, and Dacheng Tao. Learning from models beyond fine-tuning. *Nature Machine Intelligence*, 7(1):6–17, 2025.

Yongchao Zhou, Andrei Ioan Muresanu, Ziwen Han, Keiran Paster, Silviu Pitis, Harris Chan, and Jimmy Ba. Large language models are human-level prompt engineers. In *The Eleventh International Conference on Learning Representations*, 2023. URL https://openreview.net/forum?id=92gvk82DE-.

Jiong Zhu, Yujun Yan, Lingxiao Zhao, Mark Heimann, Leman Akoglu, and Danai Koutra. Beyond homophily in graph neural networks: Current limitations and effective designs. In *Advances in Neural Information Processing Systems*, volume 33, pp. 7793–7804, 2020.

Qi Zhu, Natalia Ponomareva, Jiawei Han, and Bryan Perozzi. Shift-robust gnns: Overcoming the limitations of localized graph training data. *Advances in Neural Information Processing Systems*, 34, 2021.

Fuzhen Zhuang, Zhiyuan Qi, Keyu Duan, Dongbo Xi, Yongchun Zhu, Hengshu Zhu, Hui Xiong, and Qing He. A comprehensive survey on transfer learning. *Proceedings of the IEEE*, 109:43–76, 2021.

Chenyi Zi, Haihong Zhao, Xiangguo Sun, Yiqing Lin, Hong Cheng, and Jia Li. Prog: A graph prompt learning benchmark. In *The Thirty-eight Conference on Neural Information Processing Systems Datasets and Benchmarks Track*, 2024.

# Appendices

## APPENDIX CONTENTS

# A Appendix

## A.1 Reproducibility.

We have made the codebase and other implementation details available in this anonymous link: `https://anonymous.4open.science/r/UGPrompt-6C3E`

## A.2 Additional Related Work

**Prompting for LLMs.** The promising results of early LLMs Radford & Narasimhan (2018); Devlin et al. (2019) have inspired prompt tuning approaches to benefit from LLMs's reasoning capability with minimal parameter tuning. These modular methods Li & Liang (2021); Lester et al. (2021) integrate trainable prompting prefixes with LLMs, while their parameters are frozen, offering remarkable performance across various tasks and reducing complexity. Besides, Radford et al. (2019) suggested pre-training on a large and diverse corpus (WebText), demonstrating strong zero-shot performance across various tasks. Following that, Brown et al. (2020) coined the term in-context learning, which is the effort to help models, particularly LLMs, generalize to new tasks without any parameter training and only by constructing informative prompts with task descriptions, examples, and instructions. The approaches propose specific language hints to guide the reasoning process, for example, by providing fine-grained and conditioning instructions Mishra et al. (2022) or encouraging the LLM to sequential reasoning with Wei et al. (2022) or without Kojima et al. (2022) examples. Additionally, some methods iteratively score, evaluate, and update prompts in refinement loops Zhou et al. (2023); Yang et al. (2024a).

**Prompting for GNNs.** A few studies have also adopted prompt tuning for GNNs. Specifically, the main track of these works starts with the "pre-train, prompt, fine-tune" paradigm proposed by Sun et al. (2022); they addressed the common issue of discrepancy between train and test objectives that causes performance drop on the downstream application. They design a pre-training task, specifically edge prediction, that can align with the downstream task. Nonetheless, their approach is only applicable to node classification. Later, GraphPrompt Liu et al. (2023b) and GraphPrompt+ Yu et al. (2024a) propose subgraph similarity detection as a more general *task unification* for different graph tasks to pre-train a GNN encoder. Their prompting method involves task-specific trainable readout functions. Similarly, PRODIGY Huang et al. (2023) makes prompts as a combination of example subgraphs, which are connected to label nodes, and query subgraphs, which are waiting to be connected to label nodes, and they pre-train with a neighborhood matching task. Unification to subgraph classification is also proposed by GPF-Plus Fang et al. (2023) and ALL-In-One Sun et al. (2023). However, these methods resemble LLM prompting methods more from the perspective that they prompt input graphs before a frozen GNN encoder. Specifically, the former adds trainable prompting parameters to the feature matrix of an input graph, and the latter combines a subgraph with a trainable feature matrix and structure with the input. More recently, GCOPE Zhao et al. (2024) utilizes graph coordinators to align domain-shifted datasets and remedy negative transfer in cross-domain pre-training. Also, DAGPrompt Chen et al. (2025) introduces distribution-aware prompting by utilizing low-rank adaptation for heterophilic graphs. Similarly, to capture diverse node-specific patterns in non-homophilic graphs, PRONOG Yu et al. (2025b) introduces a conditional prompting. In addition, Prompting GNNs for dynamic graphs has also been studied lately Yu et al. (2025a).

There are two shortcomings with the above GNN prompting methods. First, all of them require labeled data for training their prompting functions or at test time. Second, they mostly train a new projection head/decoder for the pre-trained GNN along with the prompting parameters. However, we propose a fully unsupervised prompting method that does not involve any fine-tuning and shows its promising performance even when the competitors have access to a full or a portion of the labels.

**Consistency Regularization and Pseudo-labeling.** In the context of Semi-Supervised Learning (SSL), pseudo-labeling Lee (2013); Xie et al. (2020) and consistency regularization Bachman et al. (2014); Sajjadi et al. (2016); Laine & Aila (2017) for training neural network models when labeled data are scarce. The first technique augments the labeled set of datasets with the model's prediction on the unlabeled set, and the second one aims to minimize the discrepancy of a model's predictions on random perturbations of the same samples, which are generated by augmentation and dropout layers. Particularly, these methods have been applied for domain adaptation to mitigate the distri-

bution shift between source and target datasets Liang et al. (2020b); Kim et al. (2021). A widely studied approach to integrating pseudo-labeling and consistency regularization is to first generate random weakly and strongly augmented instances from the same samples of a dataset and then make pseudo-labels from the weakly augmented samples whenever the model makes confident predictions for them. Models are trained by these pseudo-labels as labels for the strongly augmented samples, along with labeled data if available. To select confident samples, some methods use a fixed certainty threshold Sohn et al. (2020) while others set dynamic class-wise thresholds Zhang et al. (2021); Wang et al. (2023).

Unlike previous work utilizing consistency regularization and pseudo-labeling, we are not interested in training a model or fine-tuning it. Therefore, our novelty is interpreting a prompted graph as a strongly augmented instance and utilizing the pseudo-labels of weak augmentation to train the prompting parameters.

### A.3 ALGORITHM

Algorithm 1 presents our method's prompting procedure at training time. In line 1, we initiate the base GNN's model with the pre-trained parameters tuned on the source dataset, the target dataset, the augmentation and prompting functions, and the hyperparameters of the method. We initialize the prompting parameter and fix the base GNN's parameters in lines 3-4. Line 6 shows sampling of a batch of graphs and in line 7 a strong and a weak augmentation is generated from each graph in the batch. Next, the strongly augmented graph is prompted in line 8. This prompted graph, along with the weakly augmented graph, is encoded by the GNNs encodes as in line 9. In line 10, the representation of the prompted and weakly augmented graphs is used to optimize the discriminator. Finally, in lines 9-10, the GNN's projection head (decoder) decodes the representation, and the diversity, domain adaptation, and consistency objective functions are used to optimize the prompting parameters. Algorithm 2 shows the inference stage of our method. At inference time, a test sample is passed directly to the prompting function without augmentation, and the GNN scores the prompted graph.

**Algorithm 1** UGPROMPT (Training)

1: **Input:** Target unlabeled dataset $\mathcal{D} = \{\mathcal{G}_i\}_{i=1}^{N_t}$, confidence threshold $\tau$, GNN model $\varphi = h(.;\theta_h) \circ g(.;\theta_g)$, number of trainable prompting parameters $n_p$, augmentation function $aug(.;p)$, weak augmentation probability $p_w$, and strong augmentation probability $p_s$.
2: **Output:** Prompting function $f(.;\theta_f)$ with optimized parameters $\theta^\star$.

3: Initialize prompting parameters $\theta_f$.
4: Freeze the parameters $\theta_g$ and $\theta_h$ of the base GNN.
5: **while** not converged **do**
6: Sample batch of graphs $\mathcal{B} = \{\mathcal{G}_i\}_{i=1}^{|\mathcal{B}|} \subset \mathcal{D}$.
7: For every graph $\mathcal{G} \in \mathcal{B}$ make a weak augmentation $\mathcal{G}_w \leftarrow aug(\mathcal{G}, p_w)$ and a strong augmentation $\mathcal{G}_s \leftarrow aug(\mathcal{G}, p_s)$.
8: Prompt every strongly augmented graph as $\mathcal{G}_p \leftarrow f(\mathcal{G}_s;\theta_f)$.
9: Using encoder $g$, encode every weakly augmented graph as $z_a^{\mathcal{G}} = g(\mathcal{G}_w;\theta_g)$ and every prompted graph as $z_p^{\mathcal{G}} = g(\mathcal{G}_p;\theta_g)$.
10: Pass all encodings $z_a^{\mathcal{G}}$ and $z_p^{\mathcal{G}}$ to domain discriminator and optimize its parameters $\theta_d$ by Equation (4).
11: Using decoder $h$, compute prediction scores for all encodings $z_a^{\mathcal{G}}$ and $z_p^{\mathcal{G}}$ as in Equation (1).
12: Optimize for the prompting parameters $\theta_f$ by Equation (6).
13: **end while**
14: **return** $f(.;\theta^\star)$.

### A.4 REMARK ON UGPP DEFINITION.

Firstly, our problem setting differs from out-of-distribution (OOD) generalization methods Li et al. (2023); Fan et al. (2024); Yang et al. (2024b). In OOD generalization, given samples of dataset $\mathcal{D} = \{(x_i, y_i)\}_{i=1}^{N}$ drawn from training distribution $P_{train}(X, Y)$, the goal is to train an opti-

**Algorithm 2** UGPROMPT (Inference)

**Input:** Target unlabeled dataset $\mathcal{D} = \{\mathcal{G}_i\}_{i=1}^{N_t}$, confidence threshold $\tau$, freezed pretrained GNN $\varphi = h(.;\theta_h) \circ g(.;\theta_g)$, optimized prompting function $f(.;\theta_f^\star)$
**Output:** Prediction score set $\text{PRED}_{\mathcal{D}} = \{\varphi(f(\mathcal{G}_i;\theta_f^\star);\theta_h,\theta_g); \mathcal{G}_i \in \mathcal{D}\}_{i=1}^{N_t}$

Initialize empty set $\text{PRED} = \{\}$.
**for** $\mathcal{G}_i \in \mathcal{D}$ **do**
    Directly pass $\mathcal{G}$ to $f$ and make a prompted graph as $\mathcal{G}_p \leftarrow f(\mathcal{G};\theta_f^\star)$.
    Score the prompted graph using the pre-trained GNN as $p_\varphi(y) = \varphi(\mathcal{G}_p;\theta_h,\theta_g)$
    Add $\mathcal{G}$'s score to the to the prediction set as $\text{PRED} \leftarrow \text{PRED} \cup \{p_\varphi^{\mathcal{G}}(y)\}$
**end for**
**return** PRED.

mal model $f(.;\theta)$ to have the best generalization to the test samples drawn from the distribution $P_{test}(X,Y)$, where $P_{train}(X,Y) \neq P_{test}(X,Y)$. This differs from our problem setting, as our goal is to propose a prompting method for GNNs that follows the in-context learning setting of LLMs. As discussed, LLM prompting methods commonly 1) do not retrain or fine-tune the LLM, 2) do not necessarily use labeled data, and 3) do not assume access to the data used for training the LLM. UGPP directly encourages these properties. We assume the GNN $\varphi(.;\theta_g,\theta_h)$ is first trained on distribution $\mathcal{P}_X^s\mathcal{P}_{Y|X}^s$ and $\mathcal{D}_s$ has the same train and test distributions, i.e. $\mathcal{P}_{X,Y}^{s_{train}} = \mathcal{P}_{X,Y}^{s_{test}} = \mathcal{P}_X^s\mathcal{P}_{Y|X}^s$, while this model is aimed to be used on $\mathcal{D}_t$ with unlabeled training distribution $\mathcal{P}_{X,Y}^{t_{train}}$ and test distribution $\mathcal{P}_{X,Y}^{t_{test}}$, such that $\mathcal{P}_X^{t_{train}} = \mathcal{P}_X^{t_{test}} \neq \mathcal{P}_X^s$, but $\mathcal{P}_{Y|X}^{t_{train}} = \mathcal{P}_{Y|X}^{t_{test}} = \mathcal{P}_{Y|X}^s$ and $\mathcal{P}_{Y|X}^{t_{train}}$ is not available. So far, this assumption of UGPP makes it close to the unsupervised domain adaptation (UDA) problem You et al. (2019); Farahani et al. (2021) and satisfies unsupervised learning on $\mathcal{D}_t$, the second property of LLM in-context learning methods discussed above. For the third property, we assume the source dataset $\mathcal{D}_s$ is unobservable after training, which is known as source-free domain adaptation (SFDA) Yang et al. (2021); Li et al. (2024). For the first property, we assume all the trained GNN's parameters $(\theta_g,\theta_h)$ are fixed and we do not fine-tune them on dataset $\mathcal{D}_t$, analogous to LLM in-context learning. So, our work also differs from SFDA methods, which allow fine-tuning all or a portion of the parameters on $\mathcal{D}_t$. In summary, our problem setting differs from UDA, SFDA, and OOD generalization, and it encourages evaluating and designing generalized prompting methods for GNNs.

### A.5 Additional Details on Experimental Setup

#### A.5.1 Datasets Statistics

In this work, we use datasets with different tasks and types of features. For graph classification, we evaluate on bioinformatics and molecular datasets, specifically ENZYMES Schomburg et al. (2004) for multi-class classification and DHFR Sutherland et al. (2003) for binary classification (both with continuous features), PROTEINS Borgwardt et al. (2005) with discrete features for binary classification, also on BBBP and BACE Wu et al. (2017). For node classification, we use common citation networks Cora, CiteSeer, PubMed Yang et al. (2016), and Flickr Zeng et al. (2020) with discrete features of online images for multi-class classification. We also experimented on Cornell, Texas, and Wisconsin Pei et al. (2020) as semantic web datasets with discrete features. Table 8 shows the statistics of these datasets.

#### A.5.2 Details on the Distribution Shift

Introducing distribution shift to graphs is challenging. First, the position of nodes does not matter in graphs, therefore, introducing distribution shift by geometric transformations is not an option. Second, it is hard to find invariant features among all graphs for universal manipulations to inject shift—like color manipulations in image domain since color channels are common features. Moreover, random perturbation to node features cannot be seen as a distribution shift because it may lead to noisy datasets rather than a distribution shift with some patterns. We study different distribution

Table 8: Statistic of the datasets used for experiments.

| Dataset | #Classes | #Graphs | #Nodes | #Edges | #Features | Avg. #Nodes | Avg. #Edges | Continuous Feature | Discrete Feature |
|---|---|---|---|---|---|---|---|---|---|
| ENZYMES | 6 | 600 | - | - | 21 | 32.63 | 62.14 | ✓ | ✓ |
| DHFR | 2 | 756 | - | - | 56 | 42.43 | 44.54 | ✓ | ✓ |
| PROTEINS | 2 | 1113 | - | - | 4 | 39.06 | 72.82 | ✗ | ✓ |
| BACE | 2 | 1513 | - | - | 9 | 34.1 | 73.7 | ✗ | ✓ |
| BBBP | 2 | 2050 | - | - | 9 | 23.9 | 51.6 | ✗ | ✓ |
| Cornell | 5 | 1 | 183 | 298 | 1703 | - | - | ✗ | ✓ |
| Texas | 5 | 1 | 183 | 325 | 1703 | - | - | ✗ | ✓ |
| Wisconsin | 5 | 1 | 251 | 515 | 1703 | - | - | ✗ | ✓ |
| Cora | 7 | 1 | 2708 | 10556 | 1433 | - | - | ✗ | ✓ |
| CiteSeer | 6 | 1 | 3327 | 9104 | 3703 | - | - | ✗ | ✓ |
| PubMed | 3 | 1 | 19717 | 88648 | 500 | - | - | ✗ | ✓ |
| Flickr | 7 | 1 | 89250 | 899756 | 500 | - | - | ✗ | ✓ |

shifts in the graph domain to make a comprehensive evaluation for the setting of UGPP. Here is a brief review of these distribution shifts.

**Node-level.** Previous works study two main categories of distribution shift for nodes: 1- based on added random noise to node features Knyazev et al. (2019) 2- based on structural properties such node degrees Gui et al. (2022); Yuan et al. (2023), clustering coefficient Bazhenov et al. (2023), Page Rank (PR) Bazhenov et al. (2023), and Personalized Page Rank (PPR) Zhu et al. (2021); Bazhenov et al. (2023). Because applying random noise to node features cannot necessarily represent distribution shifts, we use structural properties in our work. For that, we choose PR for main experiments as a popularity-based property since it implies challenging distribution shift Zhu et al. (2021); Bazhenov et al. (2023). We also study the clustering coefficient as a density-based property and provide results.

**Graph-level.** Apart from datasets with inherently shifted distributions **?**Ying et al. (2019); Hu et al. (2020); Ding et al. (2021); Wu et al. (2022); Gui et al. (2022), number of nodes Sui et al. (2023); Li et al. (2023), average node degrees Li et al. (2022) and other graph properties can be utilized for introducing distribution shift for graph-level tasks. However, for main experiments, we choose edge homophily ratio Zhu et al. (2020) for generating graph datasets with distribution shift because GNNs are intrinsically affected by this property for information aggregation Gilmer et al. (2017); Zhu et al. (2020); Pei et al. (2020); Lim et al. (2021), and also our experiments on common graph classification datasets show higher variance of homophily ratio among graphs of these datasets. Additionally, we evaluate our method against graph density as another distribution shift as well.

### A.5.3 EXPERIMENTAL DETAILS

**Task Unification.** A common practice for prompt tuning and in-context learning methods in graph domains is unification of different tasks Sun et al. (2022; 2023); Huang et al. (2023). However, defining a unified task in the graph domain is more challenging than in text (e.g., using LLMs), for two main reasons. First, proposing a unified task requires an enormous amount of data, labeled or unlabeled, while, in contrast to text gathering, these large graph datasets are not feasible. Second, there is a wide variety of downstream graph tasks. Nonetheless, we unify the tasks to graph classification Sun et al. (2023), considering the message-passing intrinsic of GNN Gilmer et al. (2017).

To reduce node classification to graph classification, we select the induced subgraph of each ego node within its $k$-hop neighborhood and assign the label of the ego node to this subgraph. One can also reduce edge-level tasks by selecting the $k$-hop neighborhoods around the nodes lying on the endpoints of each edge Sun et al. (2023).

**Implementation Details.** We have implemented our experiments in Pytorch Paszke et al. (2017) and used a single GPU core NVIDIA GeForce RTX 3090. To make results reliable, we run each experiment with 10 different random initializations of seeds before dataset creation and with 5 trials of model parameter initialization for every seed, which sums up to a total of 50 runs for every experiment.

We split all datasets based on properties to make a distribution shift to a 50% source dataset and a 50% target dataset. Since we split source and target datasets in the beginning in favor of making

distribution shifts, we randomly make our own train, validation, and test splits for every trial, although the node classification datasets have original splits. Therefore, the train, validation, and test split is set to 0.6, 0.1, 0.3 for graph classification datasets and to 0.3, 0.1, 0.6 for node classification datasets—to reflect more on their original splits as they have many more test examples compared to train ones. Besides, for node classification, we find the induced graphs within nodes selected from datasets after the source-target split.

We tune hyper-parameters based on the average F1 score on validation sets as follows. For we select learning rate from $\{0.01, 0.001\}$, batch size from $\{16, 32, 64\}$, number of epochs from $\{30, 50, 60\}$, loss function weights for domain adaptation and diversity $(\lambda_1, \lambda_2)$ from $\{0.25, 0.5, 0.75, 1.0, 1.25, 1.5\}$, the $L_2$ regularization factor $(\lambda_3)$ from $\{0.1, 0.2\}$, the augmentation probability $p_u$ from $\{0.1, 0.2, 0.3, 0.4, 0.5\}$ and for $p_w$ from $\{0.05, 0.1, 0.2\}$, the number of trainable prompting parameter vectors $n_p$ from $\{10, 20, 30, 50, \mathbb{E}_{N_G}\}$ where $\mathbb{E}_{N_G}$ is the average number of nodes in graphs for the graph datasets. For the certainty threshold $\tau$, we either chose a fixed threshold following FixMatch Sohn et al. (2020) or a dynamic class-wise threshold following FlexMatch Zhang et al. (2021), then we select the threshold from $\{0.1, 0.3, 0.5, 0.7\}$. The final selection of all hyper-parameters for the GCN as base GNN and for main distribution shifts (edge homophily and PR) is provided in the codes provided by the link before.

### A.6 Theoretical Analysis of UGPROMPT

We formally present the theoretical grounding for UGPROMPT by adapting the generalization bounds established by Dac in Zhang et al. (2022) for Source-Free Unsupervised Domain Adaptation (SFUDA), which our problem setting, UGPP, fundamentally belongs to.

#### A.6.1 Generalization Bound

We consider a pre-trained GNN $\varphi = h \circ g$, where $g$ is the feature encoder and $h$ is the projection head (classifier). Critically, $\varphi$ is entirely frozen in our setting. Our goal is to minimize the expected target risk (error) $\epsilon_{\mathcal{D}_t}$ by optimizing only the prompt parameters $\theta_f$:

$$\epsilon_{\mathcal{D}_t}(h_{\theta_f}) = \mathbb{P}_{\mathcal{D}_t}[h_{\theta_f}(x) \neq h^*(x)] \tag{7}$$

where $h_{\theta_f} = \varphi \circ f_{\theta_f}$ is the final prompting model, and $h^*$ is the optimal classifier. $\mathcal{D}_t$ denotes the unlabeled target domain, and we assume no access to the source domain $\mathcal{D}_s$.

We follow the findings of Theorem 3.2 of the DaC framework Zhang et al. (2022), which provides an upper bound on the target risk $\epsilon_{\mathcal{D}_t}(h)$ for adaptation methods that utilize pseudo-labeling and consistency constraints. When adapted for our prompt-based setting, the bound implies:

$$\epsilon_{\mathcal{D}_t}(\varphi \circ f) \leq \underbrace{\mathcal{O}\left(\mathbb{P}_{\mathcal{D}_t}[\varphi \circ f \neq h_{pl}] - \epsilon_{\mathcal{D}_S}(h_{pl})\right) \cdot \frac{\mathcal{R}_{\mathcal{D}_t}(\varphi \circ f)}{\gamma}}_{\text{Term 1: Consistency and Fitting Error}} + \underbrace{\max_{i \in [C]} \{d_{\mathcal{H}\Delta\mathcal{H}}(\mathcal{P}_Z^a, \mathcal{P}_Z^p)\}}_{\text{Term 2: Representation Divergence}} + \lambda \tag{8}$$

The minimization of the target risk $\epsilon_{\mathcal{D}_t}$ is achieved by designing our three loss components to serve as empirical surrogates for minimizing the primary terms in this upper bound:

- **Term 1: Pseudo-Label Fitting and Consistency Error.** $\mathbb{P}_{\mathcal{D}_t}[\varphi \circ f \neq h_{pl}]$ is the *fitting error* (the probability of disagreement with a pseudo-labeler $h_{pl}$), and $\mathcal{R}_{\mathcal{D}_t}(\varphi \circ f)$ is the *population consistency error* (model instability under input transformations $\mathcal{B}(x)$).
- **Term 2: Representation Divergence.** $d_{\mathcal{H}\Delta\mathcal{H}}(\mathcal{P}_Z^a, \mathcal{P}_Z^p)$ is the $\mathcal{H}\Delta\mathcal{H}$-Divergence between the anchor (weakly augmented sample) feature distribution ($\mathcal{P}_Z^a$) and the prompted feature distribution ($\mathcal{P}_Z^p$), measuring the effectiveness of domain alignment.

#### A.6.2 The Generalization Bound and The UGPrompt's Objectives

Our objective function $\mathcal{L} = \mathcal{L}_c + \lambda_1 \mathcal{L}_{div} + \lambda_2 \mathcal{L}_{adv}$ directly controls these terms:

**Consistency Loss ($\mathcal{L}_c$):** $\mathcal{L}_c$ empirically minimizes the combination of the fitting error and the consistency error (Term 1 in Sec. A.6.1).

$$\mathcal{L}_c = \frac{1}{|\mathcal{B}|} \sum_{\mathcal{G} \in \mathcal{B}} \mathbb{I}(\max(\tilde{p}_{\varphi}^{\mathcal{G}}(y)) > \tau) \cdot CE(\tilde{p}_{\varphi}^{\mathcal{G}}(y), \hat{p}_{\varphi}^{\mathcal{G}}(y))$$

First, $\mathcal{L}_c$ minimizes the Cross-Entropy (CE) between the confident pseudo-label $\tilde{p}_{\varphi}^{\mathcal{G}}(y)$ (derived from the weakly augmented samples) and the model's prediction for the prompted graphs $\hat{p}_{\varphi}^{\mathcal{G}}(y)$ (from $\varphi \circ f$). This forces the resulting hypothesis $\varphi \circ f$ to tightly fit the generated pseudo-labels, empirically reducing $\mathbb{P}_{\mathcal{D}_t}[\varphi \circ f \neq h_{pl}]$.

Second, $\mathcal{L}_c$ achieves prediction invariance by forcing consistency between two distinct input transformations: the weakly augmented, non-prompted input $\mathcal{G}_w$ and the strongly augmented, prompted input $\mathcal{G}_p$. This constraint directly contributes to controlling the model stability $\mathcal{R}_{\mathcal{D}_t}(\varphi \circ f)$.

**Domain Adaptation Loss ($\mathcal{L}_{adv}$):** $\mathcal{L}_{adv}$ directly serves as a surrogate loss for minimizing the divergence term. This adversarial objective forces the prompt-transformed features $\mathbf{z}_p = g(\mathcal{G}_p)$ to be indistinguishable from the anchor features $\mathbf{z}_a = g(\mathcal{G}_w)$ by optimizing the prompt parameters $\theta_f$ against a discriminator $d$. This adversarial training minimizes a surrogate for the $\mathcal{H}\Delta\mathcal{H}$-Divergence (Term 2 in Sec. A.6.1). By aligning the generated features $\mathcal{P}_Z^p$ back towards the anchor distribution $\mathcal{P}_Z^a$, we ensure the prompt efficiently mitigates the covariate shift without pushing the features into OOD regions outside the core knowledge of the frozen encoder $g$.

**Diversity Loss ($\mathcal{L}_{div}$):** The diversity term $\mathcal{L}_{div} = -\lambda_1 H(\hat{q})$ (maximizing the entropy of the average prediction $\hat{q}$) serves as a necessary regularizer. This objective prevents the model from collapsing all predictions into a single dominant class, a trivial solution that minimizes $\mathcal{L}_c$ but invalidates the classifier. This ensures the optimal parameters $\theta_f^*$ lead to a non-degenerate hypothesis $\varphi \circ f$ that preserves the inherent discriminability learned by the frozen classifier $\varphi$.

### A.6.3 The Necessity of Universal Prompting

The success of the above approach relies on a foundational assumption about the capacity of the minimal prompt $f_{\theta_f}$. The DaC framework assumes the adaptation mechanism (fine-tuning a deep $\phi$) is functionally powerful enough to capture any shift. Since our deep GNN $\varphi$ is frozen, the burden of handling the entire graph shift falls solely on the shallow prompt $f_{\theta_f}$.

The universality of our feature-only prompt, justified by Theorem 1 of GPF-Plus derivation Fang et al. (2023), acts as the theoretical guarantee. Essentially, UGPrompt's feature-based prompting function $f_{\theta_f}$ is universally capable of mathematically simulating the effect of any arbitrary graph-level structural or feature transformation on the final feature representation $\mathbf{Z}$. This capacity guarantees that even if the covariate shift is structural, the prompt $f_{\theta_f}$ has the functional power to generate the minimally required input perturbation $\mathcal{G}_p$ that successfully aligns the feature distributions ($\mathcal{P}_Z^p \approx \mathcal{P}_Z^a$), thus guaranteeing the feasibility of minimizing the divergence term (Term 2 of 8) across all possible graph shifts.

The combination of the strong SFUDA generalization bound (from DaC Zhang et al. (2022)) and the proven universal capacity (from GPF-Plus Fang et al. (2023)) provides a comprehensive theoretical justification for the UGPrompt architecture.

## A.7 Additional Experimental Results

### A.7.1 Comparison with More baselines

To validate whether UGPrompt with no label constraint can offer practical advantages over few-shot methods, in this section, we evaluate our method against more recent state-of-the-art models, namely DAGPrompt, PRONOG, and GCOPE. As evidenced in Tables 9 and 10, UGPrompt generally outperforms the few-shot baselines in new experiments.

Specifically, UGPrompt consistently surpasses all baselines on graph classification and achieves competitive (first or second best) results on node classification. The robustness of zero-label acts as

Table 9: Comparison against methods specialized for few-shot learning on graph classification under distribution shift. UGPROMPT (with 0% labels) consistently outperforms few-shot competitors (with 25% labels), which often suffer catastrophic negative transfer.

| Method | %Label | ENZYMES | PROTEINS | DHFR | BBBP | BACE |
|---|---|---|---|---|---|---|
| DAGPrompt | 25 | -47.6 | -36.4 | -9.3 | -3.1 | -7.0 |
| PRONOG | | -26.8 | -26.6 | -2.1 | 0.0 | 9.8 |
| GCOPE | | -28.5 | -15.8 | -6.2 | -3.5 | -15.2 |
| **UGPROMPT (ours)** | **0** | **2.9** | **8.1** | **2.0** | **1.1** | **10.4** |

Table 10: Comparison against methods specialized for few-shot learning on node classification under distribution shift. Few-shot methods achieve the highest gain on most datasets, but UGPROMPT is the best overall performer without relying on any labeled data.

| Method | %Label | Cora | CiteSeer | PubMed | Flickr | Cornell | Texas | Wisconsin |
|---|---|---|---|---|---|---|---|---|
| DAGPrompt | 25 | 3.2 | 1.0 | **16.3** | **16.4** | **25.1** | **37.7** | **15.1** |
| PRONOG | | -7.1 | -3.9 | -5.3 | -26.7 | -3.7 | 34.3 | 4.4 |
| GCOPE | | 0.4 | -4.5 | -2.4 | -30.9 | -14.1 | -6.8 | -3.9 |
| **UGPROMPT (ours)** | **0** | **6.5** | **3.6** | 7.2 | 6.1 | 21.5 | 13.6 | 11.1 |

a powerful regularizer, forcing distribution alignment for positive transfer, which contrasts sharply with few-shot methods that often suffer from catastrophic negative transfer and overfitting to biased samples under distribution shifts. In addition, UGPROMPT has notably less complex (lower number of trainable parameters) than the baselines. Therefore, heavier models like DAGPrompt (which has separate trainable low-rank matrices for each input and GNN encoder layer) fail catastrophically on smaller graph classification datasets—despite having superior performance on large and heterophilic node classification tasks—and undesirably show negative improvement as it requires a larger number of samples.

### A.7.2 EFFECTIVENESS ACROSS DIFFERENT DISTRIBUTION SHIFTS.

The problem setup UGPP validates how well prompting methods can relieve the performance drop of a GNN facing distribution shift. Therefore, we aim to show the generalization of UGPROMPT across different kinds of distribution shifts. Previously, we evaluated our method on distribution shift based on edge homophily ratio and Page Rank (PR). Here we add shifts based on graph density for graph classification and clustering coefficient for node classification.

*Graph Density Distribution Shift.* Table 11 illustrates UGPROMPT generally attains the best results on the graph datasets with consistent positive performance gain, while the competitors mostly have negative performance gain on DHFR and PROTEINS in all cases even when they take advantage of 50% of labeled data of the target distribution. Besides, we have the second-best performance on ENZYMES after Fine-tuning in 50% label setting while beating this baseline in 25% label setting.

*Node Clustering Coefficient Density Distribution Shift.* The results in Table 12 reflect on the superiority of UGPROMPT over all competitors on CiteSeer and PubMed. However, GPF-Plus outperforms our method on Cora when it has access to 50% of labeled samples while is beaten by UGPROMPT when 25% of labels are available. Notably, we excel over all of the baselines on PubMed with a high margin and with no labels.

### A.7.3 GENERALIZATION TO ADVANCED GNN BACKBONES

A core principle of a prompting method is that it should be agnostic to the specific GNN backbone, demonstrating effectiveness across a range of architectures. To validate this, we extend our experiments beyond the foundational GCN and GAT models by incorporating two powerful, recent GNNs as suggested by the reviewer. We specifically chose: 1) GATv2 Brody et al. (2022), a model that uses dynamic attention to better handle graphs with varying levels of homophily and heterophily. 2) GraphGPS Rampasek et al. (2022), a graph transformer that uses a global attention mechanism to address common GNN challenges like oversmoothing and oversquashing.

The results of these new experiments are presented in Table 13 for graph and node classification tasks, respectively. The findings clearly demonstrate that our method, UGPROMPT, consistently outperforms all baselines when applied to these advanced GNN backbones. This is particularly

Table 11: Graph classification results for GCN as the base model on target datasets having distribution shift based on graph density. Overall, the best results are attained by UGPROMPT without any labels of the target dataset compared to the case where baselines have access to 50% of labels.

| Method | %Label | ENZYMES | | PROTEINS | | DHFR | |
|---|---|---|---|---|---|---|---|
| | | F1 | IMP | F1 | IMP | F1 | IMP |
| BaseModel | 0 | 39.1$^{\pm 4.1}$ | 0.0 | 56.1$^{\pm 4.0}$ | 0.0 | 76.3$^{\pm 3.8}$ | 0.0 |
| Fine-Tuning | 50 | **40.7**$^{\pm 0.7}$ | **4.1** | 39.5$^{\pm 1.6}$ | -29.6 | 76.6$^{\pm 0.2}$ | 0.4 |
| GraphPrompt | | 33.6$^{\pm 1.4}$ | -14.1 | 55.7$^{\pm 0.9}$ | -0.7 | 58.3$^{\pm 3.1}$ | -23.6 |
| All-In-One | | 30.0$^{\pm 3.2}$ | -23.3 | 37.3$^{\pm 9.5}$ | -33.5 | 77.2$^{\pm 0.7}$ | 1.2 |
| GPF-Plus | | 39.2$^{\pm 1.4}$ | 0.3 | 57.6$^{\pm 1.2}$ | 2.7 | 74.2$^{\pm 0.9}$ | -2.8 |
| Fine-Tuning | 25 | 38.0$^{\pm 1.1}$ | -2.8 | 37.0$^{\pm 3.6}$ | -34.0 | 73.6$^{\pm 0.5}$ | -3.5 |
| GraphPrompt | | 29.9$^{\pm 1.4}$ | -23.5 | 53.3$^{\pm 1.8}$ | -5.0 | 57.8$^{\pm 3.1}$ | -24.2 |
| All-In-One | | 27.3$^{\pm 3.8}$ | -30.2 | 34.2$^{\pm 10.7}$ | -39.0 | 77.1$^{\pm 0.7}$ | 1.0 |
| GPF-Plus | | 39.1$^{\pm 1.3}$ | 0.0 | 57.2$^{\pm 1.7}$ | 2.0 | 74.2$^{\pm 0.9}$ | -2.8 |
| UGPROMPT (ours) | **0** | 40.0$^{\pm 1.0}$ | 2.3 | **58.3**$^{\pm 0.8}$ | **3.9** | **78.0**$^{\pm 0.8}$ | **2.2** |

Table 12: Node classification results for GCN as the base model on target datasets having distribution shift based on node clustering coefficient. When 50% of target dataset labels are visible to baseline, the unsupervised UGPROMPT achieves the second-best results while it performs the best overall datasets in cases where 25% of labels are available for competitors.

| Method | %Label | Cora | | CiteSeer | | PubMed | |
|---|---|---|---|---|---|---|---|
| | | F1 | IMP | F1 | IMP | F1 | IMP |
| BaseModel | 0 | 59.0$^{\pm 3.1}$ | 0.0 | 44.1$^{\pm 1.6}$ | 0.0 | 60.0$^{\pm 0.8}$ | 0.0 |
| Fine-Tuning | 50 | 60.2$^{\pm 0.9}$ | 2.0 | 38.7$^{\pm 0.5}$ | -12.2 | 53.5$^{\pm 2.3}$ | -10.8 |
| GraphPrompt | | 59.9$^{\pm 0.3}$ | 1.5 | 44.8$^{\pm 0.3}$ | -1.6 | 61.3$^{\pm 0.1}$ | 2.2 |
| GPPT | | 47.9$^{\pm 6.8}$ | -18.8 | 39.0$^{\pm 2.2}$ | -11.6 | 55.1$^{\pm 3.7}$ | -8.2 |
| All-In-One | | 53.7$^{\pm 1.2}$ | -9.0 | 39.4$^{\pm 1.0}$ | -10.7 | 47.1$^{\pm 0.7}$ | -21.5 |
| GPF-Plus | | **61.4**$^{\pm 0.6}$ | **4.1** | 41.7$^{\pm 0.6}$ | -5.6 | 61.3$^{\pm 1.0}$ | 2.2 |
| Fine-Tuning | 25 | 56.5$^{\pm 0.6}$ | -4.2 | 39.9$^{\pm 0.4}$ | -9.5 | 48.7$^{\pm 3.9}$ | -18.8 |
| GraphPrompt | | 58.0$^{\pm 0.4}$ | -1.7 | 43.7$^{\pm 0.3}$ | -0.9 | 61.3$^{\pm 0.1}$ | -2.2 |
| GPPT | | 46.4$^{\pm 4.6}$ | -21.4 | 38.2$^{\pm 2.9}$ | -13.4 | 54.5$^{\pm 3.6}$ | -9.2 |
| All-In-One | | 53.7$^{\pm 1.0}$ | -9.0 | 38.3$^{\pm 0.9}$ | -13.2 | 48.9$^{\pm 0.8}$ | -18.5 |
| GPF-Plus | | 59.8$^{\pm 0.5}$ | 1.4 | 40.3$^{\pm 0.6}$ | -8.6 | 60.9$^{\pm 0.8}$ | 1.5 |
| UGPROMPT (ours) | **0** | 60.5$^{\pm 0.3}$ | 2.5 | **45.1**$^{\pm 0.4}$ | **2.3** | **64.7**$^{\pm 0.3}$ | **7.8** |

noteworthy as the baselines retain the significant advantage of access to labeled data from the target domain, whereas our method operates in a completely unsupervised manner. These results confirm that the effectiveness of our prompting framework is not dependent on a specific GNN architecture and that it generalizes robustly to more powerful and modern backbones.

### A.7.4 COMPARISON WITH SOURCE-FREE DOMAIN ADAPTATION METHODS

While our problem setup is distinct from SFDA methods, the shared goal of adapting a model without source data motivates a direct empirical comparison. To this end, we evaluate UGPROMPT against two recent, state-of-the-art graph SFDA methods: SOGAMao et al. (2024b) and GraphCTAZhang et al. (2024). Since these methods are designed for node classification, we conduct the evaluation on our node classification datasets.

To create a fair comparison within our prompting-focused problem setup, we adapt these baselines. SFDA methods typically fine-tune the entire model; instead, we align them with the "lightweight fine-tuning" paradigm common to other baselines by freezing the pre-trained GNN's encoder and only allowing the decoder (prediction head) to be trained on the target data. This contrasts with our method, UGPROMPT, where both the encoder and decoder remain fully frozen.

The results of this comparison are presented in Table 14. UGPROMPT consistently and significantly outperforms both adapted SFDA methods across all datasets. This outcome is powerful, as it demonstrates that our parameter-efficient approach of training only a prompt is more effective for adaptation than the more common strategy of fine-tuning the prediction head. In addition, our

Table 13: Graph classification results for GraphGPS and GATv2 as the base model on target datasets having distribution shift based on node clustering coefficient. UGPROMPT achieves almost the best across all datasets without labels, while 25% of labels are available for competitors.

| BaseGNN | Method | %Label | BBBP | | BACE | | Cornell | | Texas | | Wisconsin | |
|---|---|---|---|---|---|---|---|---|---|---|---|---|
| | | | F1 | IMP | F1 | IMP | F1 | IMP | F1 | IMP | F1 | IMP |
| GraphGPS | BaseModel | 0 | 87.0 | - | 73.0 | - | 22.8 | - | 24.4 | - | 20.8 | - |
| | Fine-Tuning | 25 | 87.8 | 0.8 | 70.0 | -4.1 | 24.8 | 8.8 | 27.0 | 10.7 | 19.6 | -5.8 |
| | GraphPrompt+ | | 77.8 | -10.6 | 51.5 | -29.5 | 12.7 | -44.3 | 22.8 | -6.6 | 5.9 | -71.6 |
| | All-In-One | | 72.1 | -17.1 | 39.5 | -46.9 | 19.6 | -14.0 | 0.3 | -98.8 | 22.3 | 7.2 |
| | GPF-Plus | | 87.7 | 0.8 | 73.6 | 0.8 | 22.9 | 0.4 | 26.9 | 10.2 | 22.5 | 8.2 |
| | UGPROMPT (ours) | **0** | **88.6** | **1.8** | **75.0** | **2.7** | **26.6** | **16.7** | **28.2** | **15.6** | **23.1** | **11.1** |
| GATv2 | BaseModel | 0 | 88.8 | - | 63.8 | - | 16.0 | - | 22.0 | - | 24.7 | - |
| | Fine-Tuning | 25 | 89.4 | 0.7 | 67.8 | 6.3 | 17.8 | 11.3 | 22.3 | 1.4 | 23.5 | -4.9 |
| | GraphPrompt+ | | 83.6 | -5.9 | 64.3 | 0.8 | 10.3 | -35.6 | 2.0 | -90.9 | 8.2 | -66.8 |
| | All-In-One | | 88.5 | -0.3 | 47.4 | -25.7 | 18.6 | 16.3 | 16.6 | -24.5 | 16.9 | -31.6 |
| | GPF-Plus | | 89.3 | 0.6 | **68.6** | **7.5** | 18.2 | 13.8 | 21.8 | -0.9 | 25.4 | 2.8 |
| | UGPROMPT (ours) | **0** | **89.6** | **0.9** | 67.9 | 6.4 | **20.2** | **26.3** | **23.0** | **4.5** | **26.2** | **6.1** |

Table 14: Comparison again unsupervised SFDA methods. UGPROMPT outperforms both competitors while it has significantly less number of trainable parameters.

| Method | Label | Cora | | CiteSeer | | PubMed | | Flickr | |
|---|---|---|---|---|---|---|---|---|---|
| | | F1 | IMP | F1 | IMP | F1 | IMP | F1 | IMP |
| Base Model | - | 53.8 | - | 44.1 | - | 57.1 | - | 16.5 | - |
| SOGA | 0% | 53.1 | -1.3 | 43.7 | -0.9 | 54.9 | -3.9 | 14.5 | -12.1 |
| GraphCTA | | 49.2 | -8.6 | 38.0 | -13.8 | 12.1 | -78.8 | OOM | OOM |
| UGPROMPT (ours) | 0% | **57.3** | **6.5** | **45.7** | **3.6** | **61.2** | **7.2** | **17.5** | **6.1** |

method is significantly lighter since we only train a small set of trainable prompting vectors, but these methods are originally proposed to fine-tune all parameters of the pretrained model.

### A.7.5 EMBEDDING DISTRIBUTION ANALYSIS UNDER DISTRIBUTION SHIFT

Figure 3 illustrates the distribution of embeddings produced by the base GNN's encoder for the PubMed dataset. The setting is for PR distribution shift with GCN as the base GNN. It compares the embeddings for the BaseModels on source (BaseModel-source) and target (BaseModel-Target) test data when graphs are not prompted in both cases. Additionally, it shows the embeddings for

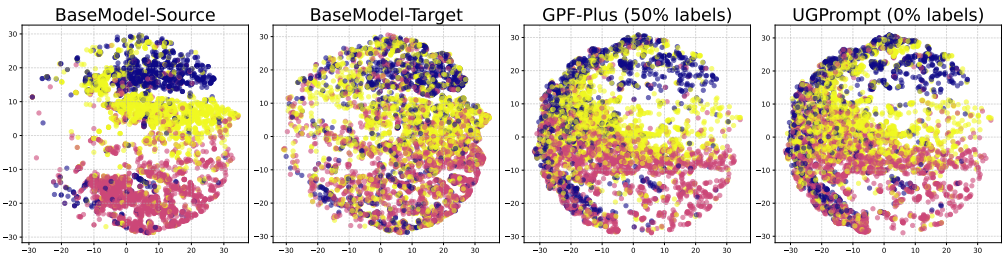


Figure 3: Distribution of embeddings generated by the base GNN encoder on the PubMed dataset under PR distribution shift with GCN as the base GNN. Embeddings for BaseModel on source and target test data without prompting and embeddings for UGPROMPT and GPF-Plus when target test graphs are prompted are presented. This highlights UGPROMPT 's ability to mitigate distribution shift without labeled data, producing well-separated representations similar to the source distribution.

Table 15: Statistic of the datasets used for experiments.

| Dataset | #Samples | NE | IR | IMP% of Diversity Reg. | IMP% of Domain Reg. |
|---|---|---|---|---|---|
| ENZYMES | 300 | 0.997 | 1.26 | 1.5 | 1.2 |
| PROTEINS | 556 | 0.949 | 1.72 | 6.6 | 4.3 |
| DHFR | 378 | 0.980 | 1.39 | 0.0 | 0.7 |
| Cora | 1354 | 0.941 | 4.72 | 4.0 | 0.7 |
| CiteSeer | 1663 | 0.965 | 1.94 | 1.3 | 0.0 |
| PubMed | 9858 | 0.966 | 1.91 | 0.2 | 0.0 |

UGPROMPT and GPF-Plus when graphs from the target test data are prompted, while UGPROMPT is fully unsupervised and GPF-Plus consumes 50% of labeled data.

This figure provides empirical evidence supporting our claims. First, UGPROMPT, which employs consistency regularization without labeled data, achieves equal or better performance in mitigating distribution shift compared to GPF-Plus although the latter has access to labeled data. Second, when using confident pseudo-labels and keeping the GNN's parameters fixed after pre-training, the prompting function aligns with the knowledge learned from the source data. This approach preserves samples within densely homophilous regions while pushing uncertain samples (those in overlapping regions) away, replicating the source data distribution as seen in BaseModel-Source. As a result, the method produces well-separated representations, enabling the projection head to effectively discriminate between classes using the same pre-trained weights.

### A.7.6 EFFECT OF REGULARIZATION METHODS

We study the effect of domain adaptation and diversity regularization methods introduced in Section 3.2. Minimizing the entropy of the score's expected value (as a diversity regularization term) has also been used in prior representation learning studies Hu et al. (2017); Liang et al. (2020a). This regularization term relieves the harmful effect of class imbalance. Meanwhile, the domain adaptation regularization term is more beneficial for smaller datasets since inferring their distribution from a low number of samples is difficult, making the chances of generating OOD prompted graphs higher. To showcase the effect of these objective terms, we first introduce two common methods of measuring class imbalance that are the Imbalanced Ratio (IR) and Normalized Entropy (NE). A higher IR and a lower NE show more class imbalance in the datasets. Denoting the frequency of each class of a dataset as $f_i$, while we have $C$ classes, IR and NE are defined as below:

$$IR = \frac{f_{max}}{f_{min}}; \qquad f_{min} = \arg\min_i f_i, \quad f_{max} = \arg\max_i f_i \tag{9}$$

$$NE = \frac{H}{log(C)}; \qquad H = -\sum_{i=1}^{C} p_i log(p_i), \quad p_i = \frac{f_i}{\sum_{i=1}^{C} f_i} \tag{10}$$

Tables 15 shows the total number of samples in the target datasets (50% of the actual dataset sizes because we split the datasets into half source and half target), the statistics of their corresponding test sets, and the IMP% of UGPROMPT on these datasets (we fix GCN as the base GNN).

When looking at both graph and node classification results, the general trends support our claims that the regularization methods have a positive impact. The first main trend observed in each task group is that diversity regularization is more effective as dataset imbalance increases; specifically, on PROTEINS and Cora, which are the most imbalanced datasets for graph and node classification respectively, diversity regularization shows the highest IMP%. Furthermore, when considering dataset size, domain regularization generally demonstrates its greatest effect on smaller datasets. For example, Cora, the node classification dataset with the fewest samples, benefits the most from domain regularization. An exception regarding domain regularization's effect might be seen when comparing PROTEINS with DHFR and ENZYMES; this could be because PROTEINS has discrete features, whereas ENZYMES and DHFR also include continuous features, potentially reducing the impact of domain regularization.

Table 16: Ablation study on the contribution of each objective function ($\lambda_1$ and $\lambda_2$ are respectively the weights of diversity and domain adaptation objectives as in Equation 6) while using GCN as the base model. Both objectives show positive effect on UGPROMPT's performance.

| **Dataset** | Base ($\lambda_1$, $\lambda_2$=0.0) | | | | | | |
|---|---|---|---|---|---|---|---|
| **Cora** | **F1=56.3** | $\lambda_1$ | 0.25 | 0.5 | 0.75 | 1.0 | 1.25 | 1.5 |
| | | **IMP%** | 1.4 | 1.6 | 2.0 | 2.0 | 2.0 | 2.0 |
| | | $\lambda_2$ | 0.25 | 0.5 | 0.75 | 1.0 | 1.25 | 1.5 |
| | | **IMP%** | 1.2 | 1.1 | 1.1 | 0.9 | 0.9 | 1.1 |
| **PROTEINS** | **F1=51.0** | $\lambda_1$ | 0.25 | 0.5 | 0.75 | 1.0 | 1.25 | 1.5 |
| | | **IMP%** | 3.1 | 5.9 | 7.1 | 7.5 | 7.5 | 7.5 |
| | | $\lambda_2$ | 0.25 | 0.5 | 0.75 | 1.0 | 1.25 | 1.5 |
| | | **IMP%** | 4.1 | 5.1 | 6.3 | 6.3 | 6.5 | 6.9 |

Table 17: Performance comparison of different methods across various source (S) and target (T) datasets.

| **Method** | **%Label** | **Cora** | | **CiteSeer** | | **PubMed** | | **ENZYMES** | | **PROTEINS** | | **DHFR** | |
|---|---|---|---|---|---|---|---|---|---|---|---|---|---|
| | | **F1(S)** | **F1(T)** | **F1(S)** | **F1(T)** | **F1(S)** | **F1(T)** | **F1(S)** | **F1(T)** | **F1(S)** | **F1(T)** | **F1(S)** | **F1(T)** |
| Base Model | - | 75.5 | 53.8 | 63.1 | 44.1 | **81.9** | 57.1 | 49.5 | 47.7 | 60.5 | 51.8 | 78.2 | 75.5 |
| Fine-Tuning | 25 | 69.8 | 51.7 | 57.2 | 40.0 | 74.2 | 54.3 | 43.4 | 46.4 | 56.2 | 47.5 | **79.4** | 76.8 |
| UGPROMPT (ours) | **0** | **75.7** | **57.3** | **63.3** | **45.7** | 81.0 | **61.2** | **49.6** | **49.1** | **63.3** | **56.0** | 78.5 | **77.0** |

Table 18: Performance comparison of UGPROMPT against the competitor under no distribution shift. An overall assessment across all datasets shows superior performance of our unsupervised method.

| **Method** | **Label** | **Cora** | | **CiteSeer** | | **PubMed** | | **ENZYMES** | | **PROTEINS** | | **DHFR** | |
|---|---|---|---|---|---|---|---|---|---|---|---|---|---|
| | | **F1** | **IMP** | **F1** | **IMP** | **F1** | **IMP** | **F1** | **IMP** | **F1** | **IMP** | **F1** | **IMP** |
| Base Model | | 64.9 | - | 50.5 | - | 73.2 | - | 54.5 | - | 51.8 | - | 75.1 | - |
| GraphPrompt+ | 25 | **72.6** | **11.9** | 48.8 | -3.4 | **76.4** | **4.4** | 57.1 | 4.8 | 35.2 | -32.2 | 55.4 | -26.3 |
| GPF-Plus | | 66.5 | 2.5 | 51.2 | 1.4 | 73.6 | 0.5 | 57.9 | 6.2 | 49.5 | -4.4 | 76.1 | 1.3 |
| UGPROMPT (ours) | **0** | 65.9 | 1.5 | **51.4** | **1.8** | 75.8 | 3.6 | **58.7** | **7.7** | **52.2** | **0.8** | **76.2** | **1.5** |

To better show the effect of each regularization methods, we also do a more comprehensive ablation study on Cora and PROTEINS as the representatives of datasets for node and graph classification. Table 16 shows how increasing the weight of each regularization term, as in Equation 6, improves the performance on both datasets, especially on PROTEINS.

### A.7.7 EFFECTIVENESS UNDER NO DISTRIBUTION SHIFT

A key concern for any adaptation method is whether adapting to a new target distribution causes "catastrophic forgetting," degrading performance on the original source domain. To measure this, we adapted models on the target data (with a distribution shift) and then evaluated their performance on both the original source test set and the target test set. The results are presented in Table 17, with columns marked (S) for source and (T) for target evaluation. The findings show that UGPROMPT not only adapts effectively to the target distribution but also maintains higher performance on the source data compared to traditional lightweight fine-tuning, demonstrating its robustness against catastrophic forgetting.

To further understand our method's behavior, we also investigated its effect in a no-shift setting, where the model is prompted for a target domain that shares the same distribution as the source. As shown in Table 18, we measured the F1 score improvement (IMP) over the base model in this scenario. The results demonstrate that UGPROMPT consistently improves performance even without a distribution shift. This benefit is more evident than that of competing baselines, which show smaller gains and occasionally fail to improve performance at all. This indicates that our prompting approach serves as a general performance enhancer, not just a tool for mitigating distribution shifts.

Table 19: The effect of the number of trainable prompting vectors ($n_t$) while using GCN as the base model. A higher number of trainable vectors brings marginal improvement, and the model performs favorably with a smaller number of trainable vectors.

| **Dataset** | $n_t = 10$ | $n_t = 20$ | $n_t = 30$ | $n_t = 40$ | $n_t = 50$ | $n_t = 60$ |
|---|---|---|---|---|---|---|
| **Cora** | 57.3 | 57.2 | 57.3 | 57.4 | 57.4 | 57.5 |
| **PROTEINS** | 55.5 | 56.0 | 56.1 | 55.8 | 56.7 | 56.2 |

Table 20: Comparison of UGPROMPT with other prompting methods based on the average full dataset training and test (inference) time measures in seconds. UGPROMPT has marginally higher training time and a test time below the average of all methods.

| **Method** | **Cora** | | **CiteSeer** | | **PubMed** | | **Flickr** | |
|---|---|---|---|---|---|---|---|---|
| | Test time (s), 813 nodes | Train time (s), 406 nodes | Test time (s), 984 nodes | Train time (s), 492 nodes | Test time (s), 5917 nodes | Train time (s), 2957 nodes | Test time (s), 22313 nodes | Train time (s), 17850 nodes |
| Fine-Tuning | 0.075 | 0.077 | 0.096 | 0.052 | 1.081 | 0.636 | 1.833 | 1.585 |
| All-In-One | 1.638 | 0.746 | 0.452 | 0.26 | 7.016 | 3.933 | 10.782 | 9.856 |
| GraphPrompt+ | 0.715 | 0.802 | 0.166 | 0.197 | 4.206 | 4.970 | 2.243 | 4.094 |
| GPF-Plus | 0.939 | 0.766 | 0.351 | 0.275 | 5.542 | 3.754 | 7.494 | 9.479 |
| UGPrompt **(ours)** | 0.925 | 1.181 | 0.315 | 0.458 | 5.56 | 4.946 | 6.730 | 13.904 |
| Average across Prompting Methods | 1.054 | 0.874 | 0.321 | 0.298 | 5.581 | 4.401 | 6.812 | 9.333 |

### A.7.8 EFFECT OF THE NUMBER OF TRAINABLE PROMPTING VECTORS

As the final ablation study, we evaluate the effect of increasing the number of trainable prompting vectors. For this experiment, we also fix GCN as the base GNN and report the results in Table 19. This empirical evaluation clarifies that increasing the number of does not have a significant impact on UGPROMPT's performance. This conclusion is indeed favorable meaning that our method can achieve desirable results even with considerably low number of trainable parameters.

### A.7.9 ANALYSIS OF COMPUTATIONAL COST

A practical consideration for any adaptation method is its computational cost. The unsupervised nature of UGPROMPT, which relies on data augmentation and multiple regularization components, introduces a manageable overhead during the training phase. This is an expected trade-off for the significant advantage of operating without labeled data. Table 20 shows the seconds of the average full dataset training epoch time and test time across node classification datasets. Our training times are marginally higher than supervised prompting baselines, but scale reasonably on large graphs like PubMed and Flickr.

However, the more critical metric for real-world deployment is inference efficiency. Once the prompt is trained, the adaptation process is complete. At test time, the expensive training components, such as data augmentation and the discriminator, are no longer required. The inference step simply involves a forward pass through the frozen GNN with the learned prompt, resulting in a computational complexity of $O(NLd^2 + L|E|d + NdN^*)$—as discussed in Section 3.3—compared to $O(NLd^2 + L|E|d)$ of a regular GNN models and $N^*$ is number of trainable prompting vectors. Since, in all our experiments, even for large graphs $N^* \leq 50$, the overhead can be neglected. Our empirical results confirm this efficiency, showing that UGPROMPT's test time is consistently below the average of competing prompting methods, making it a lightweight and practical solution for deployment.

### A.7.10 EFFECT OF CHANGING THE PROMPTING FUNCTION

An advantage of UGPROMPT, as discussed in Section 3.1, is its versatility, as it serves as a general framework agnostic to the base GNN and the prompting function. This means our unsupervised framework can potentially enhance a prefix prompting function such as Fang et al. (2023); Sun et al. (2023). To support this claim, we design an experiment where we substitute our experimental prompting function (which is similar to GPF-Plus) with All-In-One's prompting function and present the results in Table 21. These results show how the performance of All-In-One's prompting improves when integrated into our framework. Notably, this improvement occurs without using labeled data.

Table 21: Evaluation of UGPROMPT with All-In-One's prompting function using GCN as the base model. The results show that All-In-One's prompting function performs better when wrapped in our unsupervised framework, demonstrating that UGPROMPT is a versatile prompting framework capable of enhancing prefix prompting methods.

| Method | %Label | ENZYMES | | PROTEINS | | DHFR | |
|---|---|---|---|---|---|---|---|
| | | F1 | IMP | F1 | IMP | F1 | IMP |
| BaseModel | 0 | $47.7^{\pm 5.7}$ | - | **51.8**$^{\pm 7.0}$ | - | $75.5^{\pm 6.3}$ | - |
| All-In-One | 50 | $\underline{48.7}^{\pm 1.0}$ | $\underline{2.1}$ | $45.8^{\pm 10.4}$ | $\underline{-11.6}$ | $\underline{79.2}^{\pm 0.6}$ | $\underline{4.8}$ |
| | 25 | $45.8^{\pm 1.9}$ | -4.0 | $38.1^{\pm 13.4}$ | -26.4 | $79.1^{\pm 0.6}$ | 4.6 |
| UGPROMPT (ours) | **0** | **48.9**$^{\pm 0.9}$ | **2.5** | $\underline{50.8}^{\pm 2.5}$ | **-1.9** | **79.3**$^{\pm 2.4}$ | **5.0** |

Table 22: Augmentation type's effect on UGPROMPT performance using GPF-Plus's feature prompting function. Feature augmentation aligns more with the prompting function and generally achieves better results.

| Method | Aug. Type | ENZYMES | | PROTEINS | | DHFR | | Cora | | CiteSeer | | PubMed | |
|---|---|---|---|---|---|---|---|---|---|---|---|---|---|
| | | F1 | IMP | F1 | IMP | F1 | IMP | F1 | IMP | F1 | IMP | F1 | IMP |
| BaseModel | | 47.7 | - | 51.8 | - | 75.5 | - | 53.8 | - | 44.1 | - | 57.1 | - |
| UGPROMPT (ours) | Feature | **49.1** | **2.9** | **56.0** | **8.1** | **77.0** | **2.0** | **57.3** | **6.5** | **45.6** | **2.9** | **61.0** | **6.8** |
| | Structural | 48.2 | 1.0 | 54.5 | 5.2 | 75.2 | -0.4 | 57.0 | 5.9 | 44.8 | 1.6 | 55.7 | -2.5 |

### A.7.11 EFFECT OF TYPES OF AUGMENTATION

Augmentation is a key component of our framework. As discussed in Section 3.1, the type of augmentation should align with the prompting function. For instance, if the prompting function applies feature modifications, as in our main experimental prompting function, feature augmentation is expected to be more beneficial than structural augmentation (e.g., adding or removing edges), and vice versa.

As an ablation study on the type of augmentation Table 22 shows how different types of augmentation impact UGPROMPT's performance. Here our prompting function transforms the feature matrix, the feature augmentation masks features, and structural augmentation drops edges. Results meet our expectations that the feature augmentation attains better performance since it aligns better with the prompting function. Since none of the existing GNN prompting functions can be categorized solely as structural prompting (without changing the node representations), we leave experimenting with such prompting method for future works.

### A.7.12 UNSUPERVISED PROMPTING VS FULLY SUPERVISED PROMPTING

Since UGPROMPT accomplishes significant improvements in different experiments, we are interested in evaluating the competitors while allowing them to access 50%, 75%, and 100% of labeled data from target distributions. We show the results of these settings in Tables 23 and 24, and Figures 4 and 5. All the results are reported for both GCN and GAT when we have distribution shifts based on edge homophily for graph classification and PR node classification.

Graph classification results for both GCN and GAT base models in Tables 23 illustrate the superior performance of UGPROMPT as an unsupervised method compared to the baselines in most cases, while they are given the advantage to access 50% of labeled samples for training on the target datasets. On the node classification datasets, UGPROMPT achieves the second-best performance as shown in Table 24. Specifically discussing larger node classification datasets, it is noteworthy that we beat all the baselines on Flickr and only underperform GraphPrompt+ on PubMed.

Observing Figure 4 when we use GAT as the base model, UGPROMPT outperforms GPF-Plus and GraphPrompt on graph classification datasets even when they utilize fully labeled target datasets. *This clearly shows the effectiveness of our proposed method,* UGPROMPT. Additionally, we achieve closely competitive results with GCN as the base model in 100% label setting overall. Besides looking at the node classification results for both GNNs, we generally obtain the second-best improvement in 75% label setting and perform favorably with 100% compared to the best baseline.

Table 23: Graph classification results on target datasets for GCN as the base model. Our unsupervised method mostly achieves the best results even when the competitors use 50% of the labeled data.

| Base GNN | Method | %Label | ENZYMES | | PROTEINS | | DHFR | |
|---|---|---|---|---|---|---|---|---|
| | | | F1 | IMP | F1 | IMP | F1 | IMP |
| GCN | BaseModel | 0 | 47.7$^{\pm 5.7}$ | - | 51.8$^{\pm 7.0}$ | - | 75.5$^{\pm 6.3}$ | - |
| | Fine-Tuning | 50 | 45.0$^{\pm 2.0}$ | -5.7 | 46.9$^{\pm 1.6}$ | -9.5 | 77.6$^{\pm 0.2}$ | 2.8 |
| | GraphPrompt | | 40.2$^{\pm 1.5}$ | -15.7 | 54.1$^{\pm 1.0}$ | 4.4 | 73.1$^{\pm 0.9}$ | -3.2 |
| | GraphPrompt+ | | 29.7$^{\pm 1.7}$ | -37.7 | 49.7$^{\pm 1.0}$ | -4.1 | 65.5$^{\pm 1.3}$ | -13.2 |
| | All-In-One | | 48.7$^{\pm 1.0}$ | 2.1 | 45.8$^{\pm 10.4}$ | -11.6 | **79.2**$^{\pm 0.6}$ | **4.8** |
| | GPF-Plus | | 48.6$^{\pm 0.9}$ | 1.9 | 53.8$^{\pm 2.4}$ | 3.9 | 77.4$^{\pm 0.3}$ | 2.5 |
| | UGPROMPT (ours) | **0** | **49.1**$^{\pm 0.6}$ | **2.9** | **56.0**$^{\pm 1.5}$ | **8.1** | 77.0$^{\pm 2.4}$ | 2.0 |
| GAT | BaseModel | 0 | 44.1$^{\pm 6.4}$ | - | 51.5$^{\pm 8.1}$ | - | 77.3$^{\pm 3.5}$ | - |
| | Fine-Tuning | 50 | 43.3$^{\pm 1.2}$ | -1.8 | 49.2$^{\pm 0.5}$ | -4.5 | 78.0$^{\pm 0.2}$ | 0.9 |
| | GraphPrompt | | 35.3$^{\pm 1.9}$ | -20.0 | 50.3$^{\pm 0.9}$ | -2.3 | 77.1$^{\pm 0.9}$ | -0.3 |
| | GraphPrompt+ | | 29.2$^{\pm 6.2}$ | -33.8 | 52.1$^{\pm 6.3}$ | 1.2 | 60.5$^{\pm 12.7}$ | -21.7 |
| | All-In-One | | 40.3$^{\pm 2.5}$ | -8.6 | 41.8$^{\pm 11.2}$ | -18.8 | 77.3$^{\pm 1.2}$ | 0.0 |
| | GPF-Plus | | 43.4$^{\pm 2.0}$ | -1.6 | 54.8$^{\pm 2.7}$ | 6.4 | 77.2$^{\pm 0.8}$ | -0.6 |
| | UGPROMPT (ours) | **0** | **45.9**$^{\pm 2.2}$ | **4.1** | **56.4**$^{\pm 2.0}$ | **9.5** | **78.2**$^{\pm 0.9}$ | **1.2** |

Table 24: Node classification results on target datasets for GCN as the base model. Comparing all baselines with the access to 50% of labeled data, UGPROMPT achieves the second-best results without labels.

| Base GNN | Method | %Label | Cora | | CiteSeer | | PubMed | | Flickr | |
|---|---|---|---|---|---|---|---|---|---|---|
| | | | F1 | IMP | F1 | IMP | F1 | IMP | F1 | IMP |
| GCN | BaseModel | 0 | 53.8$^{\pm 2.4}$ | - | 44.1$^{\pm 1.5}$ | - | 57.1$^{\pm 0.8}$ | - | 16.5$^{\pm 0.4}$ | - |
| | Fine-Tuning | 50 | 54.5$^{\pm 1.2}$ | 1.3 | 43.5$^{\pm 0.4}$ | -1.4 | 56.3$^{\pm 2.1}$ | -1.4 | 10.3$^{\pm 0.4}$ | -37.6 |
| | GPPT | | 50.5$^{\pm 3.1}$ | -6.1 | 40.6$^{\pm 1.2}$ | -7.9 | 51.8$^{\pm 3.7}$ | -9.3 | 13.6$^{\pm 0.5}$ | -17.6 |
| | GraphPrompt | | 55.8$^{\pm 0.3}$ | 3.7 | 43.8$^{\pm 0.3}$ | -0.7 | 57.1$^{\pm 0.1}$ | 0.0 | 13.1$^{\pm 0.2}$ | -20.6 |
| | GraphPrompt+ | | 57.3$^{\pm 0.6}$ | 6.5 | 42.9$^{\pm 0.2}$ | -2.7 | **64.9**$^{\pm 0.2}$ | **13.7** | 14.9$^{\pm 0.7}$ | -9.7 |
| | All-In-One | | 50.3$^{\pm 1.2}$ | -6.5 | 39.3$^{\pm 1.0}$ | -10.9 | 39.8$^{\pm 1.2}$ | -30.3 | 13.5$^{\pm 0.3}$ | -18.2 |
| | GPF-Plus | | **58.2**$^{\pm 0.6}$ | **8.2** | **46.8**$^{\pm 0.7}$ | **6.1** | 60.3$^{\pm 0.5}$ | 5.6 | 13.1$^{\pm 0.1}$ | -20.6 |
| | UGPROMPT (ours) | **0** | 57.3$^{\pm 0.4}$ | 6.5 | 45.7$^{\pm 0.4}$ | 3.6 | 61.2$^{\pm 0.3}$ | 7.2 | **17.5**$^{\pm 0.1}$ | **6.1** |
| GCN | BaseModel | 0 | 47.7$^{\pm 1.3}$ | - | 41.2$^{\pm 2.4}$ | - | 60.0$^{\pm 1.1}$ | - | 17.0$^{\pm 0.2}$ | - |
| | Fine-Tuning | 50 | 47.1$^{\pm 1.7}$ | -1.3 | 39.9$^{\pm 0.5}$ | -3.2 | 56.5$^{\pm 2.2}$ | -5.8 | 10.8$^{\pm 0.3}$ | -36.5 |
| | GPPT | | 32.8$^{\pm 3.8}$ | -31.2 | 35.6$^{\pm 1.2}$ | -13.6 | 51.8$^{\pm 5.5}$ | -13.7 | 13.1$^{\pm 0.3}$ | -22.9 |
| | GraphPrompt | | 48.2$^{\pm 0.5}$ | 1.0 | 40.7$^{\pm 0.3}$ | -1.2 | 60.1$^{\pm 0.1}$ | 0.2 | 13.5$^{\pm 0.1}$ | -20.6 |
| | GraphPrompt+ | | 48.2$^{\pm 0.5}$ | 1.0 | 42.0$^{\pm 0.3}$ | 1.9 | **67.1**$^{\pm 0.1}$ | **11.8** | **17.5**$^{\pm 0.6}$ | **2.9** |
| | All-In-One | | 34.6$^{\pm 4.1}$ | -27.5 | 33.0$^{\pm 1.2}$ | -19.9 | 25.4$^{\pm 5.2}$ | -57.7 | 12.5$^{\pm 0.5}$ | -26.5 |
| | GPF-Plus | | **49.6**$^{\pm 1.4}$ | **4.0** | **43.1**$^{\pm 0.6}$ | **4.6** | 60.1$^{\pm 0.5}$ | 0.2 | 13.2$^{\pm 0.2}$ | -22.4 |
| | UGPROMPT (ours) | **0** | 48.8$^{\pm 0.9}$ | 2.3 | 42.3$^{\pm 0.5}$ | 2.7 | 60.2$^{\pm 0.1}$ | 0.3 | **17.5**$^{\pm 0.1}$ | **2.9** |

Next, we evaluate our method in distribution shifts of graph density and clustering coefficient under the 75% and 100% label settings. Here we fix GCN as the base GNN. Results are in Figure 5. Similar to the previous distributions, for the graph density and clustering coefficient, UGPROMPT has a competitive or better performance on graph classification datasets and stands in second position after GPF-Plus on node classification except that our method does not see any labels.

Finally, an interesting finding of these experiments is that the competitors occasionally can cause a performance drop compared to the base models which is unexpected and undesirable. On the other hand, UGPROMPT although is an unsupervised method, does not have a negative influence on any dataset, any GNN architecture, and any type of distribution shifts. Also, all the above results can lead to the same conclusion that UGPROMPT can enhance the base GNNs which encounter different distribution shifts on various downstream tasks. Since UGPROMPT achieves promising results in a fully unsupervised manner, it offers new avenues to leverage large unlabeled datasets for improving the generalization of GNNs.

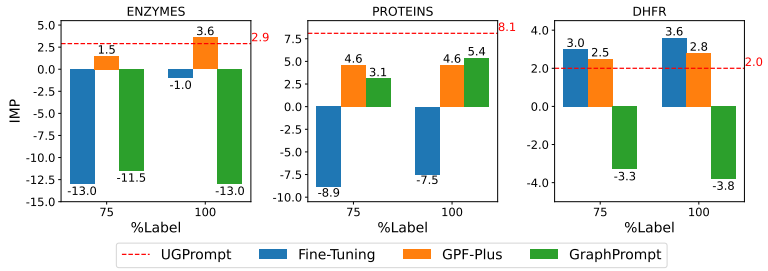


(a) Graph classification under edge homophily distribution shift for GCN as base model.

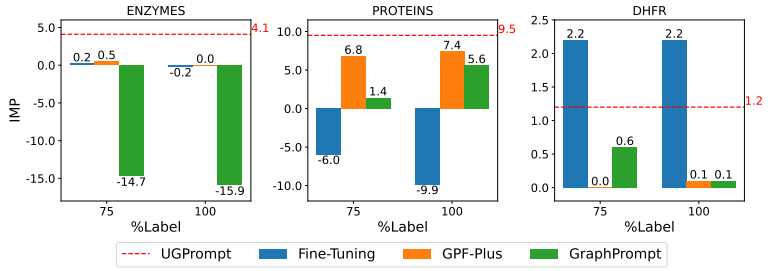


(b) Graph classification under edge homophily distribution shift for GAT as base model.

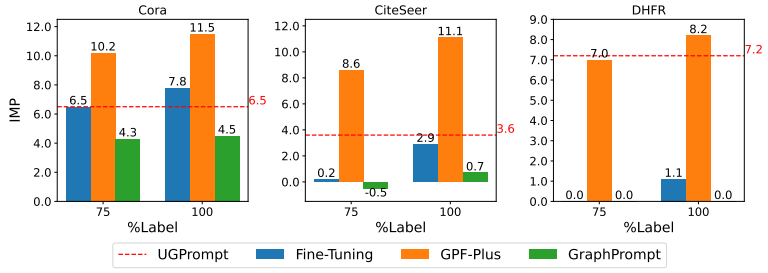


(c) Node classification under PR distribution shift for GCN as base model.

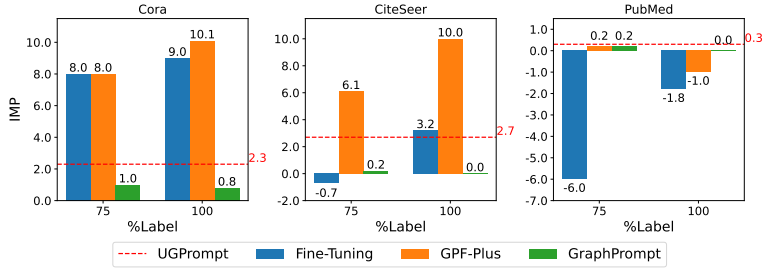


(d) Node classification under PR distribution shift for GAT as base model.

Figure 4: Performance gains for GCN and GAT base models on graph and node classification tasks in the presence of edge homophily (a, b) and node page rank (c, d) distribution shifts; where the competitor prompting methods utilize 100% and 75% labeled data of target distributions. UGPROMPT without using any labels always shows improvement over the base model and attains the best results on graph classification for GAT while having second best results in other cases.

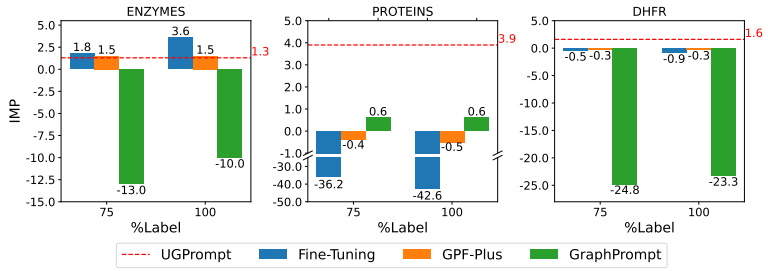


(a) Graph classification under graph density distribution shift for GCN as base model.

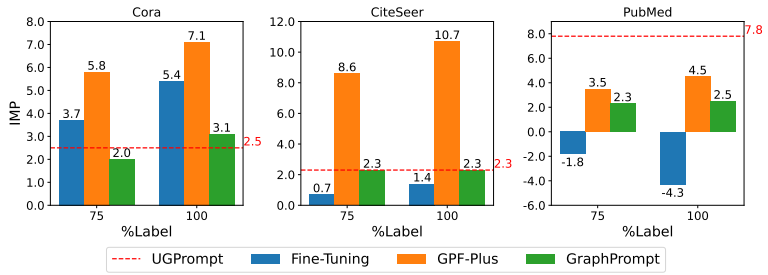


(b) Node classification under clustering coefficient distribution shift for GCN as base model.

Figure 5: Performance gains for GCN as the base model on graph and node classification tasks in the presence of graph density (a) and node clustering coefficient (b) distribution shifts when the competitor prompting methods utilize 100% and 75% labeled data of target distributions. The trend is similar to other distribution shifts (Figure 4) where UGPROMPT generally attains the best results on graph classification and the second-best on node classification.